3D modelling of the Martian North Polar Cap, using surface and sub-surface images

By:

Floris M. J. van Lieshout
0423971

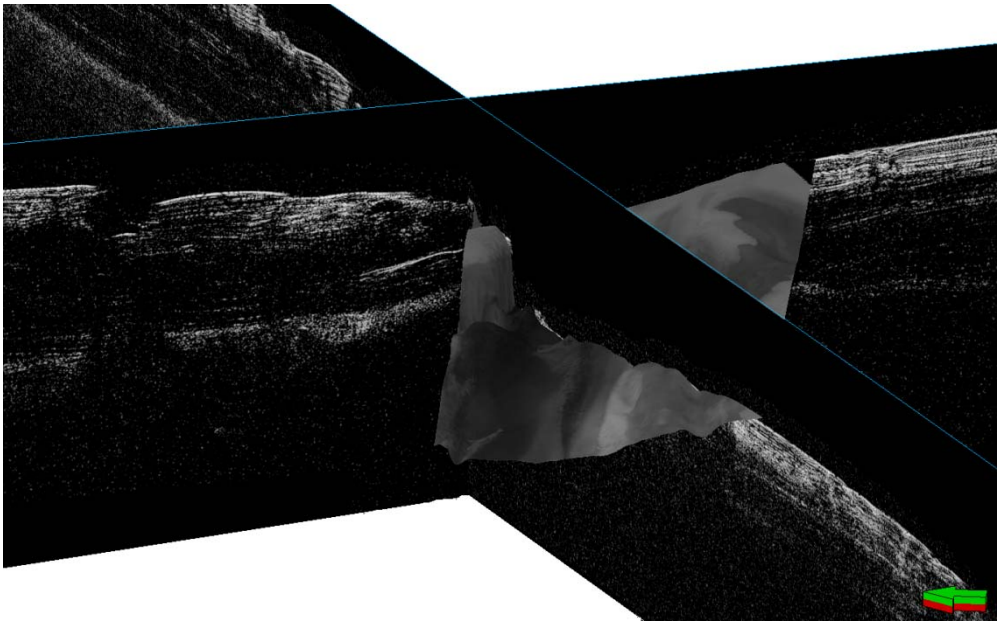

Universiteit Utrecht

Deltares
Enabling Delta Life

With the supervision of:

-TNO/Deltares, the Geological Survey of the Netherlands:
Jelmer H. P. Oosthoek & Marco H. P. Kleuskens

-Faculty of Earth Sciences, Utrecht University:
Dr. Tanja E. Zegers

Version 4.1 (28-12-2009)

Table of contents:

1. Introduction: **4**
- **Goal & Scope**
- **Nomenclature**

2. Background: **6**
- **2.1 Mars**
- **2.2 N. Pole Cap**
- **2.3 North Polar contacts**
- **2.4 Earlier research of the North Pole of Mars**
  - **2.4.1 Surface imaging**
  - **2.4.2 Radar**
  - **2.4.3 Radar + HRSC data, 3D modelling of Mars**
- **2.5 Age**
- **2.6 Scenarios**

3. Methodology: **14**
- **3.1 The Data**
- **3.2 The Instruments and Output**
  - **3.2.1 SHARAD**
  - **3.2.2 MOLA**
  - **3.2.3 HRSC**
- **3.3 Workflow**

4. Results: **21**
- **4.1 3D surface model, MOLA + HRSC**
- **4.2 Place radargram in georef. Frame**
- **4.3 Interpretation of radargrams**
  - **What is visible what not; limit of resolution**
- **4.4 Geology**
  - **4.4.1 Faults**
  - **4.4.2 Spiral Troughs**
  - **4.4.3 Layering**
  - **4.4.4 Link between SHARAD and HRSC**

5. Conclusion / Recommendations : **28**
- **5.2 Goal**
- **5.2 Problem cause**
- **5.3 Other modelling reports**
- **5.4 Scientific work with the results**
  - **5.4.1 Structural interpretation of radargrams**
  - **5.4.2 Obtaining a 3D model (incl. MOLA fit)**

6. Acknowledgements: **29**

7. Appendix: **30**

A: List of used Python scripts
B: SHARAD footprints used for modeling
C: Processing the data into usable files for Petrel.

8. References **37**

Figure on the frontpage: Surface imgae draped on MOLA and two SHARAD radargrams, 107995_r_0472302_001 and 216860_r_0656503_001.

1. Introduction:

With its valleys, volcanic mountains and two polar caps Mars shows the closest resemblance with Earth in our Solar System. Mars is therefore now an important subject of research in the planetary science. Until recently only surface information was available and not much was known about the subsurface beneath it. In 2006 subsurface radar data from the SHAllow RADar (SHARAD) imager, on board the Mars Reconnaissance Orbiter, became available (Seu et al., 2007b). With this data the internal structure of the subsurface was made visible. Till now, the best imaging gotten is from the North Pole due to the reflectivity of water. The entire ice cap from surface to the bottom of the northern ice cap has been made visible including internal layer structures. Together with surface images the North Polar Cap (NPC) has got a dense amount of data.

Combining the surface images with the radargram data to create a 3D geologic view, however, has not yet been done before.

During an internship at TNO/Deltares in Utrecht (the Netherlands) a three dimensional model of the North Polar Cap of Mars will be created. At a later stage the geological setting and the evolution of the Cap will be investigated with this model. The model will be generated by analyzing and correlating surface images of the High Resolution Stereo Camera (HRSC) and vertical radargram images of the SHARAD instrument. Both data sets will be coupled to the topographic data set of the Mars Orbital Laser Altimeter (MOLA), which will be used as a base for the model.

In this report the workflow will be described how the model is set up. In the chapter 2 a brief background will be given about the setting of Mars, its North Pole and what kind of research is already done on the NPC. Chapter 3 will give information about the data that is used during the research and how the model is build up. The workflow will not entirely be given in this chapter for it is too extended. The more detailed workflow is added as appendix. Chapter 4 and 5, respectively the results and the discussion will discuss the outcome of the model and if it is useable for scientific research in the future.

With this model, more geological aspects can be discovered and compared with other scenarios. A higher resolution will be created by using the approach of combining the subsurface and surface images. With this model it will be possible to trace layers that are visible on surface images throughout the ice cap by directly identifying them at the radargram images. This process of direct combining the subsurface and surface images has not been done before, but will give an extra dimension in the research of the Northern Polar Cap and will create a significant gain in the research of the area.

Nomenclature:

ASI Agenzia Spaziale Italiane

HRSC: High Resolution Stereo Camera, on board of the Mars Express, an ESA satellite program launched in 2003.

Mars Express: Satellite program of the ESA since 2003, so called because of the quick and efficient development time

MARSIS: Mars Advanced Radar for Subsurface and Ionosphere Sounding, on board the Mars Express

MGS: Mars Global Surveyor, a NASA satellite program launched in 1996 and ended in 2006. The satellite has got an orbit of an apoapsis of 10.107 km and a periapsis of 287 km.

MOLA: Mars Orbiter Laser Altimeter, on board of the MGS.

MRO: Mars Reconnaissance Orbiter, a NASA satellite program launched in 2005 and is still operating. NASA may even approve to continue the operation after the primary science mission has ended.

NPC: The North Polar Cap, also called Planum Boreum. The Cap represents the elevated plateau, which is build up out of the North Polar Layered Deposits (NPLD) and the underlying Basal Unit (BU).

SHARAD: Shallow (Subsurface) Radar, on board the MRO

DTM: Digital Terrain Model. Models that include information relating to surface texture in addition to information regarding elevation.

DEM: Digital Elevation Model. Models that give a representation of altitude alone

Petrel: A seismic modeling program in which seismic data can be visualized and interpreted. Eventually 3D structures can be generated and features can be added, such as surface images, density and porosity to recreate the studied area.

ArcGIS: A large collection of GIS programs that help to visualize, interpret and manage geographic information. This program can help to understand large information sets in a more efficient way.

2. Background:

2.1 An introduction to Mars

With 144.798.550 km^2 the surface of Mars is 3,5 times smaller than the surface of the Earth. It is mostly a dry and cold chaotic terrain characterised by the large old volcanic domes, craters and deep valleys.

A noticeable feature of the planet is the planetary flattening, which creates a ~20 km difference between equatorial and polar radii. The topographic map of Mars can be seen in figure 1. On this map the major topographical features are visible that define Mars. The figure shows that Mars has a very smooth and young northern hemisphere, but has a very rough and older southern hemisphere. The latter is covered by Noachian aged craters, showing the oldest rocks of Mars (Scott and Carr, 1978; Smith et al., 1999). The northern hemisphere, which lays much lower, is mostly covered by Amazonian sedimentary deposits of the Vastitas Borealis Formation (Tanaka, 2005). The cause of the dichotomy is still an unanswered question. Till now two main models can explain the origin of this dichotomy. One theory states that the northern hemisphere was renewed by plate tectonics and therefore explains the younger and smooth surface (Wilhelms and Squyres, 1984; Frey and Schultz, 1988). The other theory, however, claims one major or several impacts have altered the surface (Sleep, 1994).

Except for the chaotic and rocky terrain, Mars also has got two polar caps. The northern polar cap is slightly thicker than the southern polar cap, respectively 1,8 km and 1,5 km thick, but lies relatively much lower (Picardi et al., 2005; Plaut et al., 2007). This is due to the fact that the northern ice cap lies in a sedimentary basin in which its top lies 2 km below the zero-elevation contour. The southern ice cap lies on heavily crated terrain with its top 3 km above this contour line.

After the discovery of ice at the poles of Mars the idea that fluid water and ice played an important role in forming the Martian surface, became an important argument in later research (Masson et al., 2001; Kleinhans, 2005). New data that suggest that ice is buried within the crust, closer to the equator, concur this statement (Watters et al., 2006; Schultz, 2007; Holt et al., 2008; Boisson et al., 2009).

If a large body of water existed on the surface of the planet it is now either lost via atmospheric escape or partially resided deep in the subsurface (Clifford, 1993). As not much is known about the volume of water in the history of Mars, unfortunately therefore not much can be said about it.

The theory of atmospheric escape is based on the fact that Mars lost part of its atmosphere. This was caused by a period of intense bombardments between 4.6 and 3.8 and the loss of Mars its magnetic field (Kass and Yung, 1995). The thinned atmosphere caused the climate of the planet to cooldown quickly and become cold and dry. The average air temperatures now range now between the -83^oC and -33^oC (Hartmann, 2005), but can reach extremes of -140^oC and 20^oC. In this period of atmosphere loss also the surface water disappeared. The atmospheric pressure is at the moment less than 10 millibars composed primarily of carbon dioxide (CO_2) and minor nitrogen (N_2) and argon (Ar).

Because the planet also has an obliquity, Mars has seasons. At the moment Mars has an axial tilt of 25.2^o, but it has varied between the 11^o and 45^o. Together with the eccentricity of 0,1 they control the seasonal variations and thus also the extreme variation in temperature.

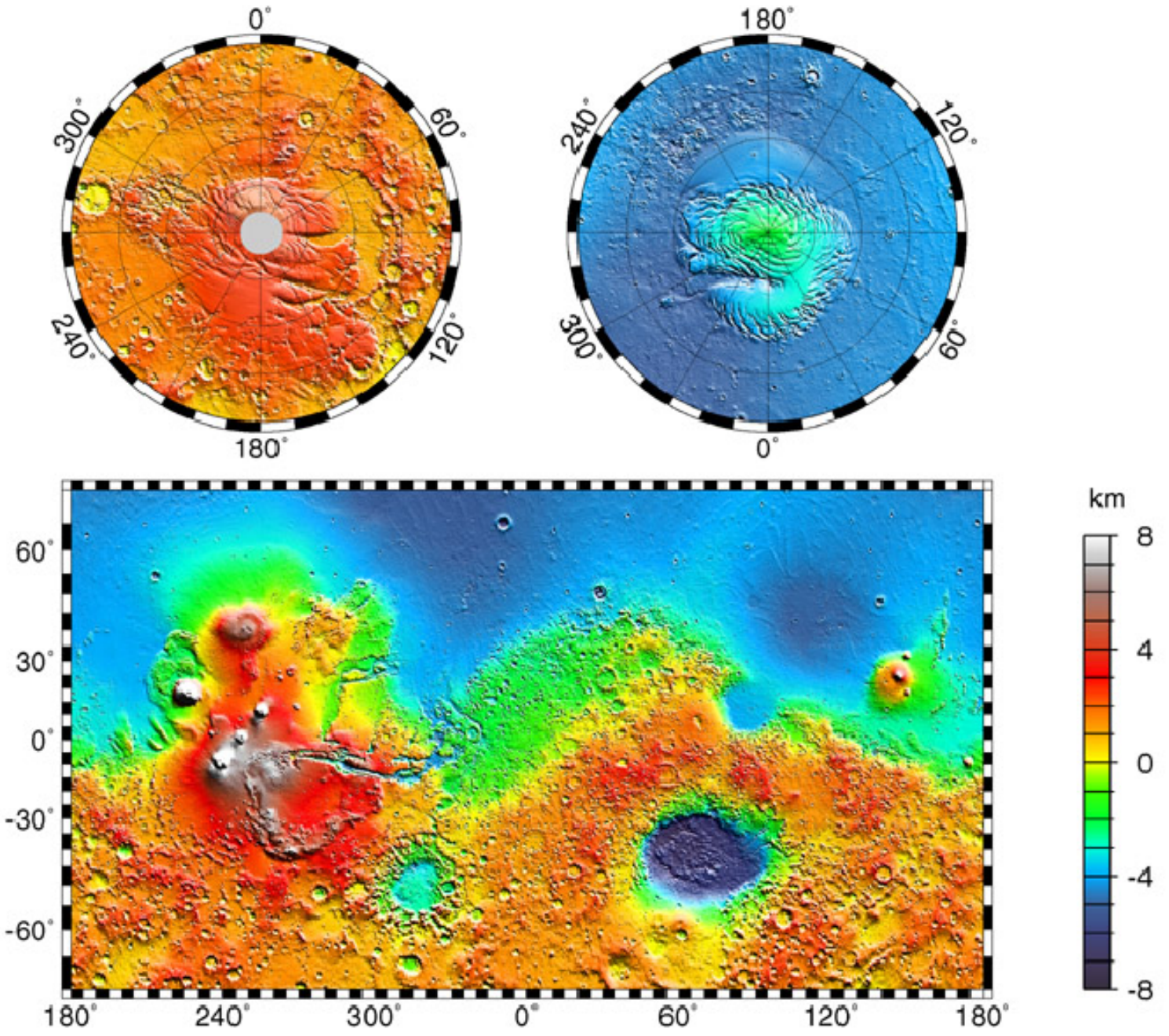

Figure 1: Topgraphical map of Mars, measured by the Mars Orbiter Laser Altimeter. Note that the volcanic mountains are higher than the scale represents.

2.2 North Pole Cap

The discovery of the North Pole of Mars was made by the British astronomer Sir William Herschel in the 18th century, who described as first the changes in width of the caps he saw. Comparing it with the Earth he suggested that this could only be ice and snow. The first photographical evidence for this, were given by the Mariner 9 and the Viking program in the '70 (Bass et al., 2000).

As said before, the North Polar Ice Cap lies in a low lying sedimentary and volcanic basin. The maximum thickness of the ice cap, called 'Planum Boreum', can be estimated at about ~1.8 km. The entire ice cap covers an area of about ~800.000 km^2 (Phillips et al., 2008). The North Polar Cap can be described as a general ice cap with a lobe structure attached to it (figure 2). This lobe and the ice cap are divided by a valley, called 'Chasma Boreale'. Many hypotheses have tried to explain how this valley was formed and what the relation is between the ice cap and the lobe. These include the formation by ablation, eolian processes and sublimation, and outflow of meltwater (Clifford, 1987; Benito et al., 1997; Anguita et al., 2000; Fishbaugh and Head, 2002). Also the large spiral troughs characterize the NPC with their structural feature. The generation of these large structures are, however, also still unknown and are therefore still subject of research e.g. Howard, 1978; Fisher, 1993; Zeng et al., 2007.

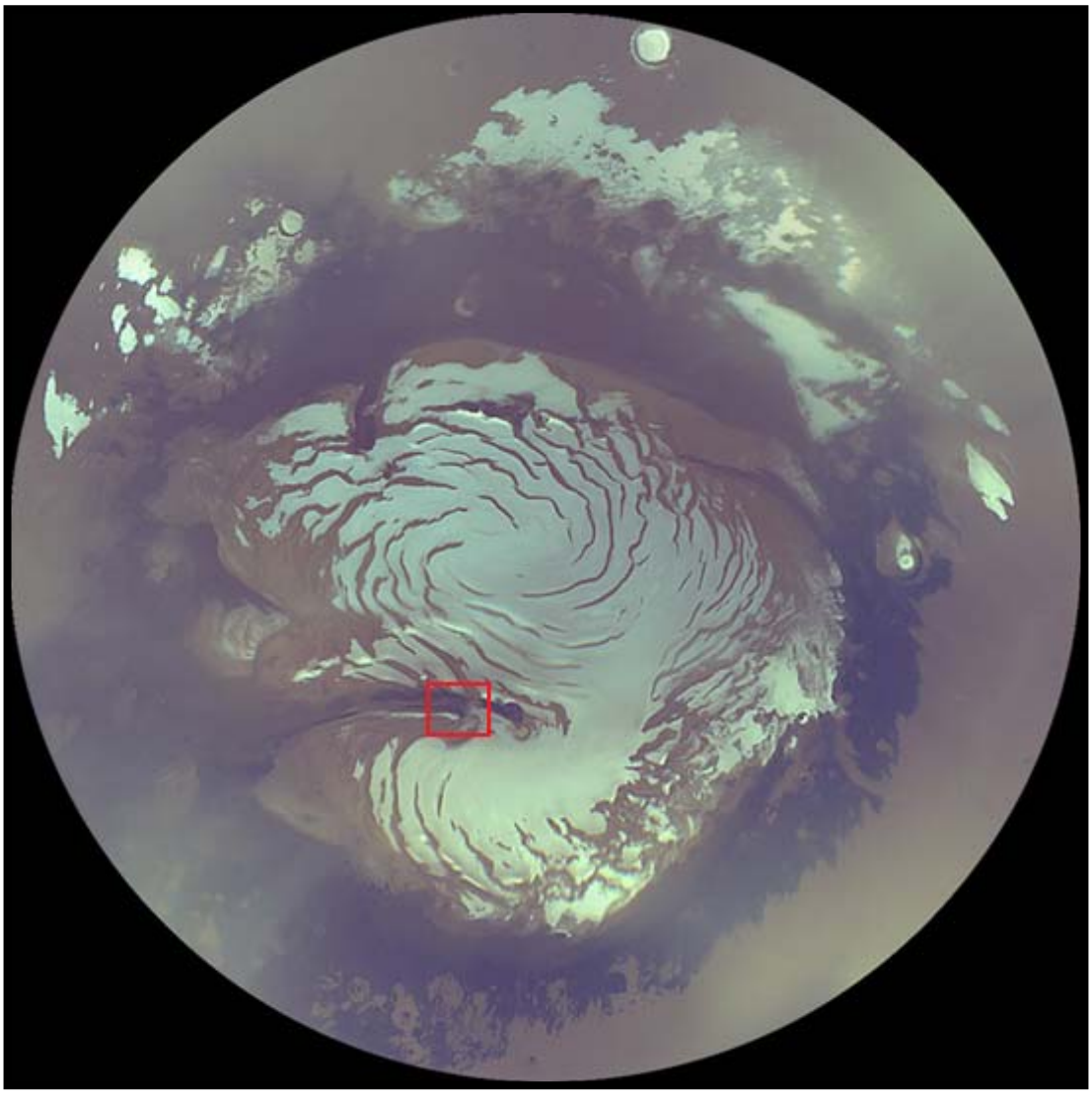

Figure 2: View of the North Polar Cap of Mars. This picture is taken by the Mars Reconnaissance Orbiter of NASA. The red lined area represents the location of figure 5a and figure 5b.

Till 2006 it was only possible to look at surface images and use the lines visible to tell something about the internal structure. Recent radargram images have made it possible to take a look inside the NPC. These images clearly show structural lines in the ice cap, and seem to represent ice layers divided by dust lines. It is thought that dust particles also contaminate the ice layers itself (Phillips et al., 2008) which leads to ice layers that do not have the properties of pure water (Hobbs et al., 1966; Heggy et al., 2006; Watters et al., 2007).
The study of this internal layering can be of great importance.
On Earth, research of Antarctica and the North Pole, by for example, the British Antarctic Survey (BAS), have shown that the internal layering of the ice caps keep a close record of the past climate fluctuation. It is thought that the internal layering of the North Polar Cap (NPC) of Mars also shows such record of recent climate changes of Mars (Schorghofer, 2008).
Recent reports in which surface and subsurface images of the NPC are studied, therefore, write about the theory that the layers that can be distinguished are all controlled by the characteristics of the Martian climate alterations (Laskar et al., 2002; Fishbaugh and Head, 2005; Levrard et al., 2007).

2.3 North Polar contacts

On bases of surface imaging studies, two major units have been identified on the North Polar Cap. The two units, respectively the North Polar Layered Deposits (NPLD) and the Basal Unit (BU), are divided by their difference in albedo and thickness of layers. This difference is probably the effect of the high sediment content of the BU and the high ice content of the NPLD (Edgett et al., 2003). In figure 3 the boundary between the NPLD and the BU can be seen. It shows a clear, sharp change from a light colored and thin layered unit to a dark colored and thick layered unit (Edgett et al., 2003; Fishbaugh and Head, 2005; Herkenhoff et al., 2007; Tanaka et al., 2008; Putzig et al., 2009a). Tanaka *et al.* (2008) made an effort in dividing these layers into more detail, based on geological and geomorphical differences, using morphologic- and composition-based data where possible. The result is a geological map with 8 different units (see figure 4).
The boundary between the ice cap and the Martian surface is formed by the contact between the Basal Unit and the Vastitas Borealis Formation (VBF), Amazonian mantle material. Unfortunately most of this contact is covered by dunes and do not show a sudden slope as can be seen at the contact between the NPLD and the BU (Tanaka and Scott, 1987).

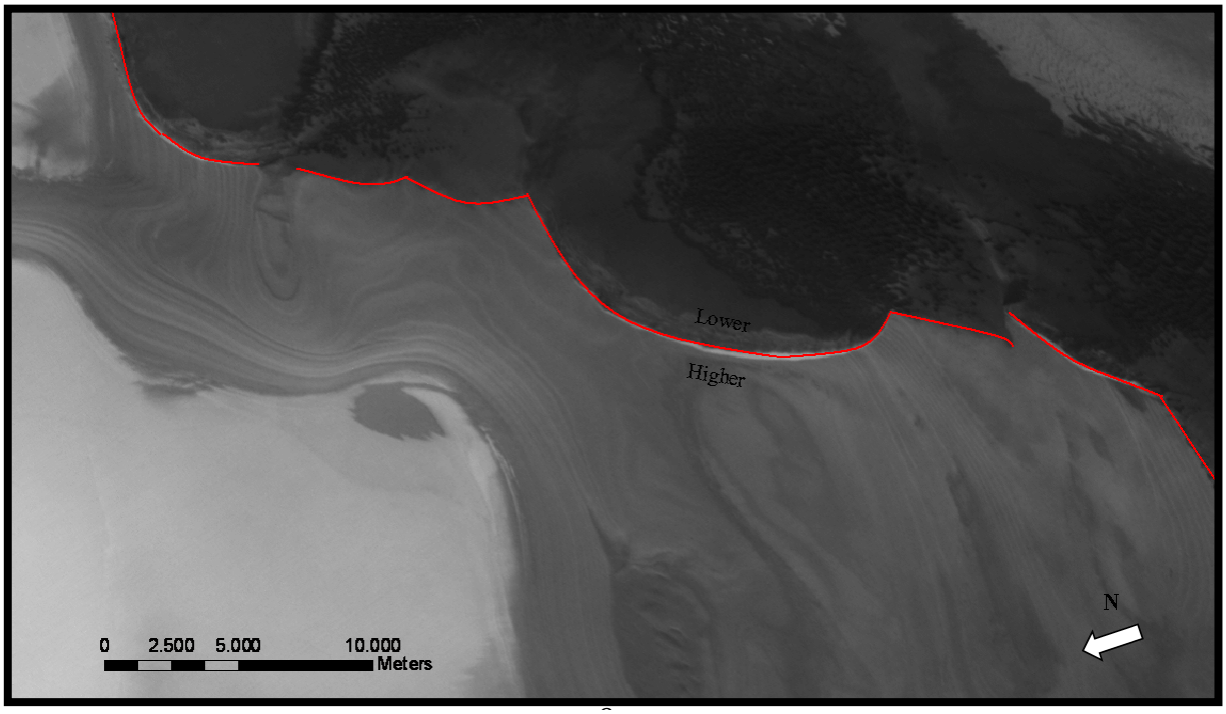

Figure 3: The contactzone between the upper layers and the lower layers of the NPC. Here a clear boundary between the light high level and the lower dark layer can be seen. The image here displays HRSC image H6007_0000_ND3.

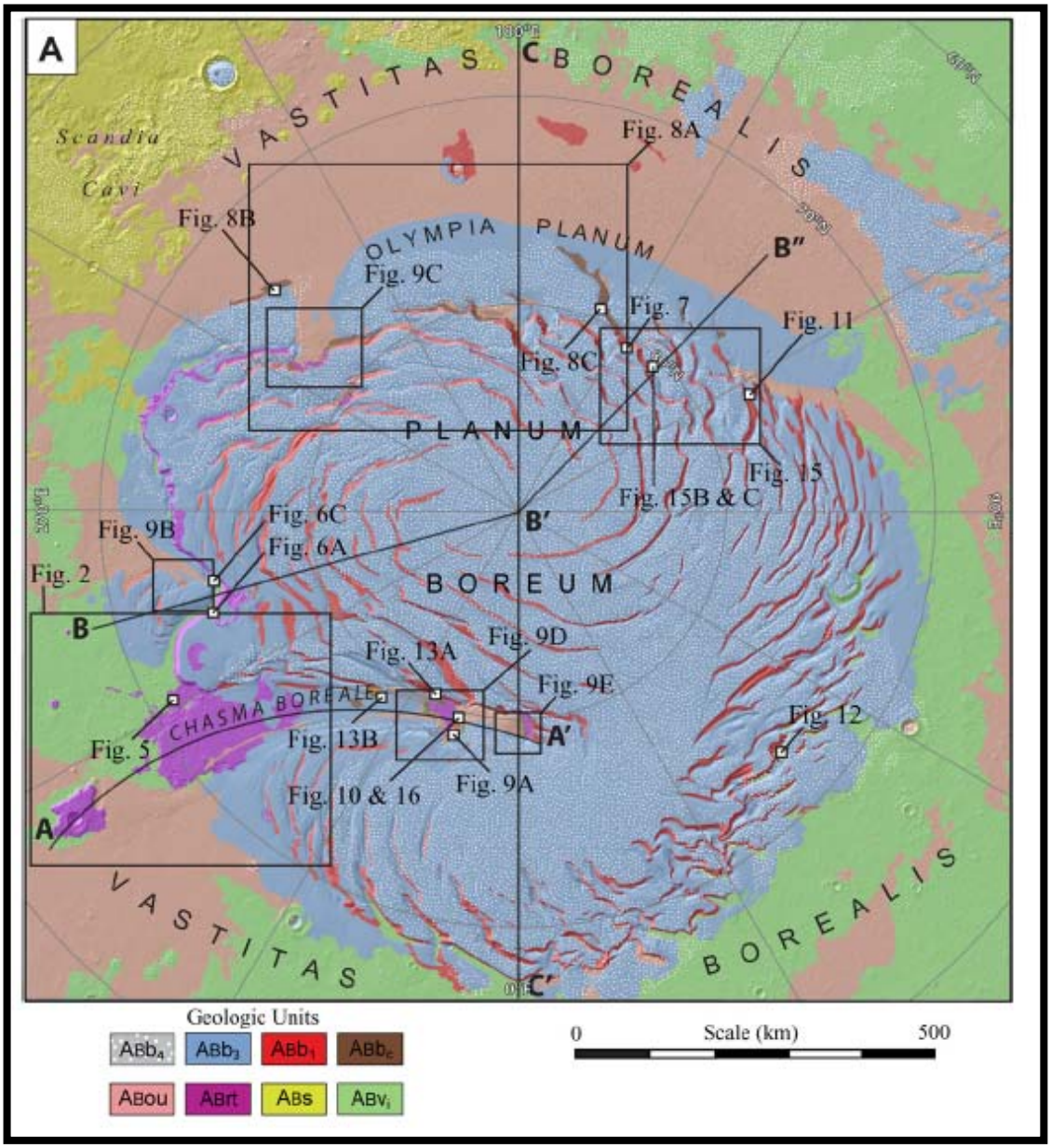

Figure 4: Figure 51: Geological Map of North Pole of Mars interpreted by Tanaka *et al.* (2008). This map is used to select the areas of which the surface images are taken.

2.4 Earlier studies of the North Pole of Mars

The research of the North Pole of Mars has been a subject of study for a few centuries now. Thanks to the topography measured by MOLA and the surface images of the Mariner 9, the Vikings 1 and 2 and the Mars Global Surveyor (MGS) much of the evolution of the ice cap has been gathered (Cutts et al., 1976; Howard et al., 1982; Weijermars, 1986; Fisher, 1993; Fishbaugh and Head, 2000). However, in these early studies low resolution images were used so only interpretations of the global structure could be made.

Much more evidence of the structure of the ice cap and its evolution has been given by the more recent missions of the Mars Reconnaissance Orbiter (MRO), the Mars Express and the Mars Global Surveyor (MGS) (Byrne, 2009; Fishbaugh et al., 2009; Milkovich et al., 2009; Perron and Huybers, 2009; Smith et al., 2009).

2.4.1 Surface imaging

The higher resolution images, given by for example the HRSC and the HiRISE instruments, show highly detailed geological features. With the use of Arc Scene the high resolution images can also be modelled into a Digital Elevation Model (DEM) as shown in figure 5a and 5b. In these figures the layers of Chasma Boreale can clearly be seen and followed in a three dimensional space. The high resolution of these images and the DEM's that can be build out of them, give the added value for science.

These image therefore form new and good evidence for new and already proposed hypothesises (Edgett et al., 2003; Heipke et al., 2004; Fishbaugh and Head, 2005; Tanaka et al., 2008; Putzig et al., 2009b). Due to these new surface images with better detail, reports have been written which state that a repeating sequence can be found in the layers (Fishbaugh and Head, 2005; Levrard et al., 2007). This structural feature could not have been described before due to the lack of resolution.

2.4.2 Radar

In 2006 radargrams imaging became available thanks to the MARSIS and SHARAD instrument. These are vertical images of the surface and subsurface showing the internal structure of the underground. These images caused a new dimension in the research of the subsurface of the Martian North Pole e.g. Plaut et al., 2007; Seu et al., 2007a; Phillips et al., 2008; Putzig et al., 2009b. Reports resulted in an enormous increase in knowledge of the internal structure of the North Pole, in which even relations are laid between the obliquity and eccentricity of Mars and the layering of the ice package.

Putzig *et al.* (2009) have used the radargrams to make a model of the North Pole by using 358 SHARAD radar images. Their report essentially concentrates on the observations of the radar images itself and the deposition centers of the different layer units found. They also mention the possibility of combining surface images with these radargrams but do not show any example of it. Until now, no other SHARAD radargram model has been made.

2.4.3 Radar + HRSC data, 3D modelling of Mars

In the last few years reports have been published in which radar images and surface images are combined e.g. Byrne, 2009; Milkovich et al., 2009. These reports show interpretations of the radargrams and the surface images individually from each other and then combining the interpretations. Their research shows that the radargrams confirm the ideas of the internal structure made when only surface imaging was available. They, however, also state that with better and more accurate data more can be said about its origin and the overall structure. A direct spatial correlation of multiple data sets will thus give more advantages for the interpretation of the North Polar Cap.

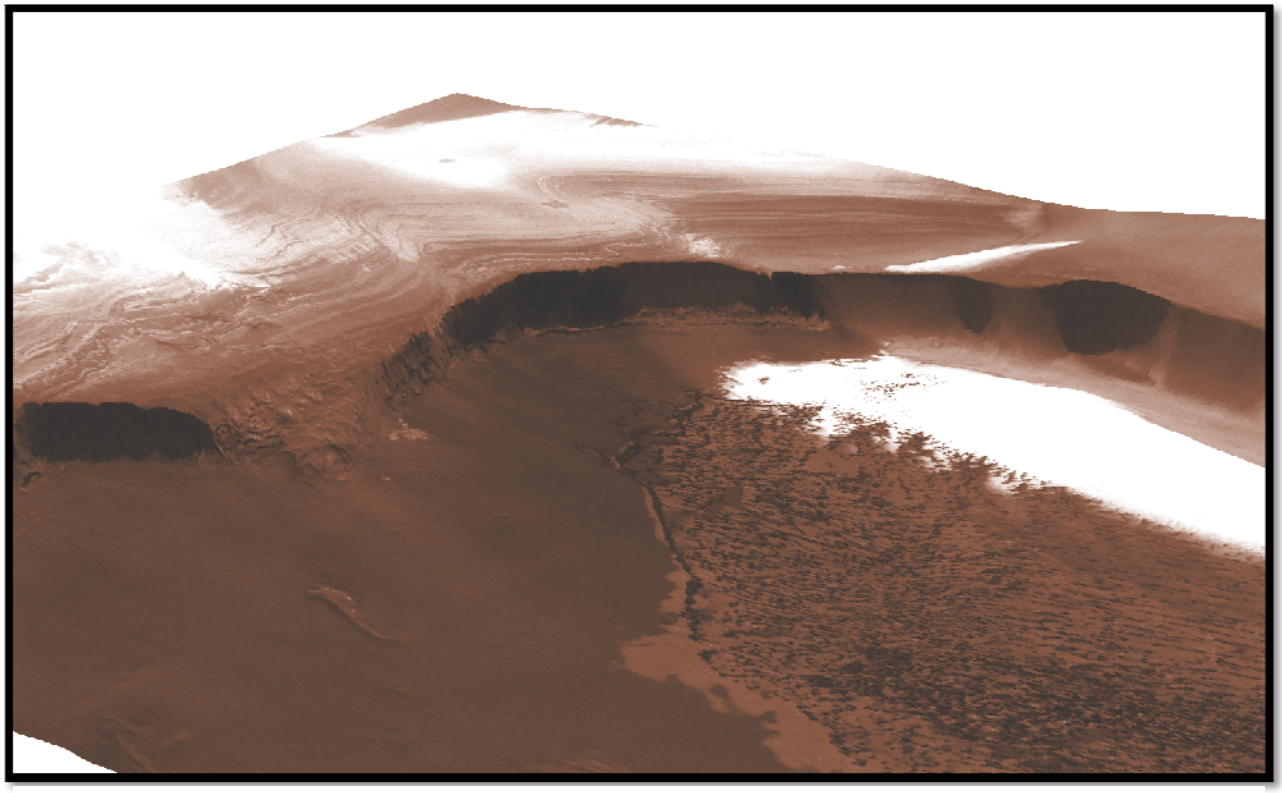

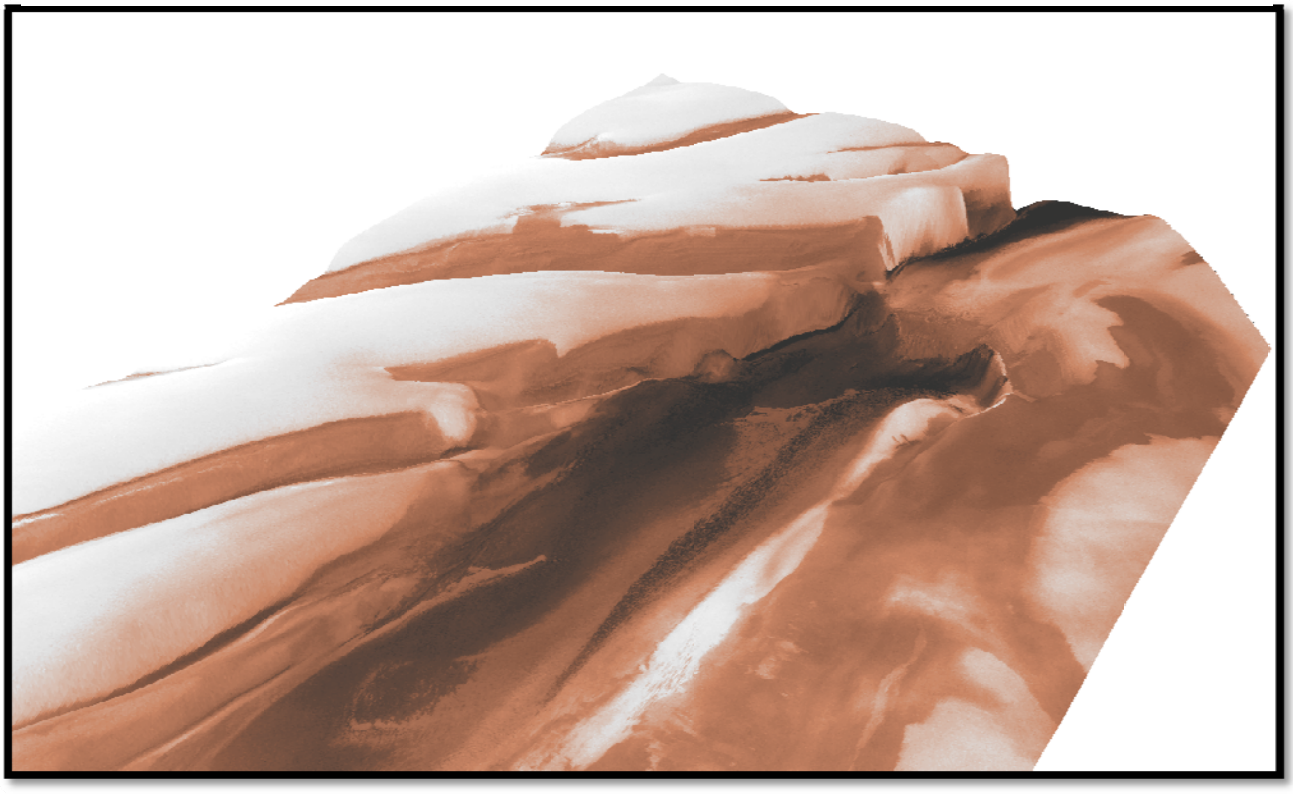

:h the sight

2.3 Age

The NPC of Mars has, Mars just like the Earth. Three Eons are distinguished: the Noachian Eon (~4.5 Gyr - 3.5 Gry), the Hesperian Eon (3.5 Gyr – 3.1 Gyr) and the Amazonian Eon (3.1 Gry till now) (Hartmann and Neukum, 2001). These Eons have been dated by correlating it to the same family of projectiles that occurred on the moon and thus the same cratering chronology (Neukum et al., 2001).
Unfortunately, because there are just a few craters found on the NPLD no exact date can be given to the ice layers, and therefore no exact time estimate can be made to determine when a structural event occurred.
Many different maximum age estimates have been stated, which makes it hard to make a strong statement of the geological evolution that occurred at the North Polar Cap. Tanaka (2008), still using cratering density based on the idea of Neukum et al., 2001, comes with an age which lies between hundreds of millions of years for the lowest layer found in the North Polar Layered Deposits (NPLD) down to 8.7 Kyr for the most upper layer of the NPLD. Levrard (2007), Phillips (2008) and Putzig (2009), however, state a maximum age of the entire NPLD of ~4.2 Myr, which is based on eccentric and oblique cyclicity.

2.4.5 Scenarios

With the new data, improved interpretations have been made of the North Polar area. Because Mars has got a close resemblance with Earth the ice cap is studied in high detail. Several scenarios therefore have been stated that describe the evolution of the North Polar Cap. One of the important issues that control the scenarios is the age of the ice cap and when all stadia occurred.

1. Putzig *et al.* (2009) state that the period of layer formation is related to the low amplitudes in oscillation of the insolation function of Levrard *et al.* (2007). They therefore accept the maximum age of the NPC of ~4.2 Ma.

2. Phillips *et al.* (2008) however look at the inter-packet zones, which correspond with the 2.4 My cycle of the eccentricity of Lascar *et al.* (2002). With this theory, which has a close resemblance with Putzig *et al.* their statement, they have calculated a maximum age of ~6.2 Ma. During accumulation periods ice is settled with a little bit dust among it. During a high or a low obliquity respectively more or less dust concentrates itself in the ice (Levrard et al., 2007).

3. Fishbaugh and Head III (2005) state that the layering of dust concentration in the ice cap is due to repeating erosion of the ice cap.
   When this process occurred is not stated, but they keep two theories open. In the first scenario the age can be very old, because the age of the underlying layer is not known. The second scenario states that the polar layers have been accumulate throughout the Amazonian.

3. Methodology:

3.1 The Data

This report focuses on the method and the resulting model, and not on a detailed interpretation of the results of model. The method used is an idea from Oosthoek & Kleuskens (Oosthoek and Kleuskens, 2009). The method is based on inserting both the radargram images of the SHARAD instrument and the surface images from the HRSC in Petrel.
Petrel is a 3D modeling program developed by Schlumberger, which is typically used in the petroleum industry. With this program we are capable to correlate multiple datasets and create a 3 dimensional geological environment. Goal of this research is therefore to insert the radargram images, the surface topography and surface images of the North Pole of Mars into Petrel and create a 3D model.
The datasets used for the research of the Northern Cap are given by the ESA, the NASA and the USGS and can be found on respectively the Planetary Science Archive FTP site, the PDS GeoScience Node site and the ftp site of the USGS (*ftp://psa.esac.esa.int/pub/mirror/MARS-EXPRESS/HRSC/MEX-M-HRSC-5-REFDR-MAPPROJECTED-V2.0/DATA/*, the *http://pds-geosciences.wustl.edu/missions/mro/sharad.htm* and *ftp://pdsimage2.wr.usgs.gov/pub/pigpen/mars/mola/polar/*). Here the data from the SHARAD, the HRSC and the MOLA can be found. The datasets can be downloaded as raw data or as modified data, which is ready to be used as input for GIS programs.
They also include reports on how they have modified the raw data. During this research the modified data sets have been used.

In the following sections the different instruments are introduced. Also the data processing and the map projection of the data will be discussed as these are two important steps in modeling with the data. For this research we make use of the June 2009 dataset of the SHARAD instrument, the HRSC instrument and the MOLA.

3.2 The Instruments and Output

3.2.1 SHARAD

The Shallow Radar (SHARAD) sounder, developed by the Agenzia Spaziale Italiene (ASI), is one of the main instruments on board the Mars Reconnaissance Orbiter (MRO). The MRO came in a 255 km x 320 km orbit of Mars at the end of 2006. The instrument his primary goal is to identify the subsurface of Mars by using a radio echo sounding technique. This technique, which is also used on Earth from aircrafts or even satellites, eventually will show the layering of the subsurface and its internal structure (Peeples et al., 1978; Siegert and Kwok, 2000; King et al., 2009).

The raw data from the instrument is processed back on Earth, at the SHARAD Operations Center (SHOC) of Alcatel Alenia Spazio (AAS) in Rome. The data is processed here to the final vertical radargram 2D-images, called 'radargrams', defined by a time-delay (vertical) versus a meter-scale (horizontal). Figure 6 shows three examples of such images.
The Mars Advanced Radar for Subsurface and Ionosphere Sounding (MARSIS) onboard the Mars Express also uses a sounder to penetrate the groundsurface of Mars. Because this sounder uses a different frequency (between 1.8 and 5.0 MHz) then the SHARAD instrument (20 MHz) it can penetrate deeper into the subsurface. The resulting images of the MARSIS, though, only show the surface and the base of icy volumes, while the SHARAD images show the near-surface internal structure. For this reason the MARSIS data is not used in this report.
The radargrams have a vertical resolution of 15m in free space (Seu et al., 2007b). The along-track footprint resolution (after synthetic aperture processing) and the cross-track resolution are respectively between 0.3-1 km and 3-6 km (Table 1). The horizontal surface resolution however, depends mainly on the surface roughness, which can play an important role in the research on the North Pole of Mars.

	Mission	*Resolution*	*Coverage*
SHARAD data	*MRO (NASA)*	The vertical resolution is 15 m in free-space and 3-6 km cross-track by 0.3-1 km along-track for horizontal resolution.	*Almost the whole Northern and Southern Pole*
MARSIS data	*Mars Express (ESA)*	A vertical resolution of 150 m in vacuum. This is 50-100 m in the subsurface	*No Coverage*
HRSC data	*Mars Express (ESA)*	A 10 m resolution with a 2 m resolution camera inside, creating full coloured 3D images	*Whole of Mars*
MOLA data	*MGS (NASA)*	The resolution can run down to 1/256 degree, which can lead to a resolution of 230 m	*Whole of Mars*

Table 1

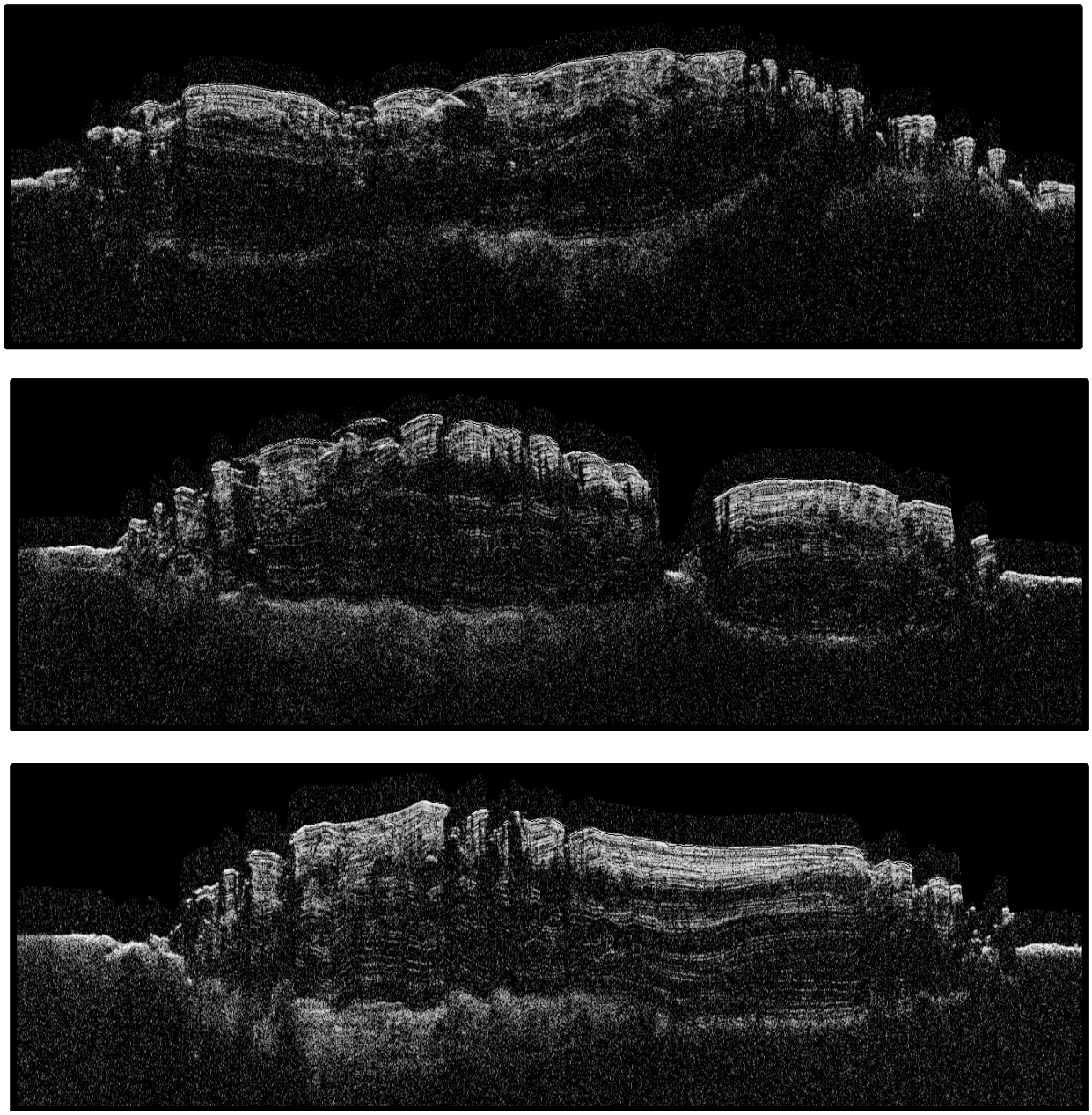

Figure 7: Radargrams taken by the SHARAD instrument. Showing respectively: 133181_r_0699002_001, 242670_r_0478402_001 and 273908_r_0614102_001.

A SHARAD image is build up out of the received reflected energy waves. These radar sounding energy waves that impinge the surface may reflect on dielectric interfaces as they cross a different media. However, not all the energy will reflect, as some of the energy will continue travelling through the subsurface towards the next reflecting interface. Essentially, there will be an energy loss until the signal is lost in the form of cosmic radio noise. For this reason the returns of the waves with increasing depth will be much weaker.
The waves that will reflect return to the instrument in a specific time-delay. With the surface and several subsurface dielectric interfaces in the ice cap the instrument will receive several echoes, all with a different time-delay. On Earth the data obtained by the MRO is processed to be projected with planetocentric coordinates and have an east-positive longitudes in the range 0^{o}–360^{o}, all with respect to the IAU 2000 reference ellipsoid (Seidelmann et al., 2002). More detailed information about the SHARAD instrument can be read in Slavney and Orosei, 2007 and Seu et al., 2007b.

3.2.2 MOLA

The Mars Orbital Laser Altimeter (MOLA) on the Mars Global Surveyor (MGS) was a mission of the NASA and the Jet Propulsion Laboratory (JPL), which was launched in 1996. Its goal was to map the topography of the Martian surface over a course of about 4 years. To make accurate measurements possible the satellite was taken into a nearly circular orbit with an altitude of 378 km. The MOLA instrument shoots ten pulses of 1,064 μm per second of infrared light at the surface and measures the time for the reflected energy to return.
All the information gathered by the MOLA was sent back to Earth and investigated at the Goddard Space Flight Center (GSFC) by the MOLA Science Team.
After 4.5 years of operating, the topography of Mars was mapped. Since then it is used as a radiometer. The final output of the data gathered shows a global rater map with a resolution of 1/256 degree, with one degree being ~59 km at the equator. At the poles the resolution will therefore be higher. The point accuracy of the MOLA can be declined to 37.5 cm in radius and a footprint of 30 meters along and across track. This, however, depend on the accuracy of the reconstruction of the radial spacecraft orbit (Smith et al., 2003).

The topographic height of the planet's surface at the footprint of the laser spot is determined by measuring the time-of-flight of the laser pulses. The topography is then determined by using the geometry of the planet radius, the spacecraft orbit altitude, and the pointing angle of the instrument (Abshire et al., 2000).
These measurements and the reconstruction of the MOLA to a coordinate system has not been done in this research, but will be briefly discussed here as it can be relevant for further understanding of the results.

To reconstruct the measurements from the MOLA instrument to a coordinate system, the pointing matrices from the attitude data are transferred to the IAU 2000 coordinate frame (Seidelmann et al., 2002). With this coordinate system a map projection of the topographical data can be made. A vertical reference frame, however, should also be taken into account. For this two reference frames can be used:

-A sphere with a radius of 3396.0 km, which is the same radius as used with the map projection.
-An aeroid, directly comparable with MOLA MEGDR grids.

The difference between the two frames can be seen in figure 7. One thus has to notice that using a different reference frame will result into a different topographic map (Gwinner et al., 2007; Rossi, 2008).
In this report, however, the polar stereographic data from the USGS is used. The data from this database uses a polar stereographic projection with the semi-minor axes of 3376200.0 and can be used as input for Arc GIS.

More about the precise setting of the MOLA from data to coordinate system can be found in the `*PEDR Data Set Information Guide'* or on the FTP-site of the USGS, respectively, *http://pds-geosciences.wustl.edu/missions/mgs/mola.htm* and ftp://pdsimage2.wr.usgs.gov/pub/pigpen/mars/mola/polar.

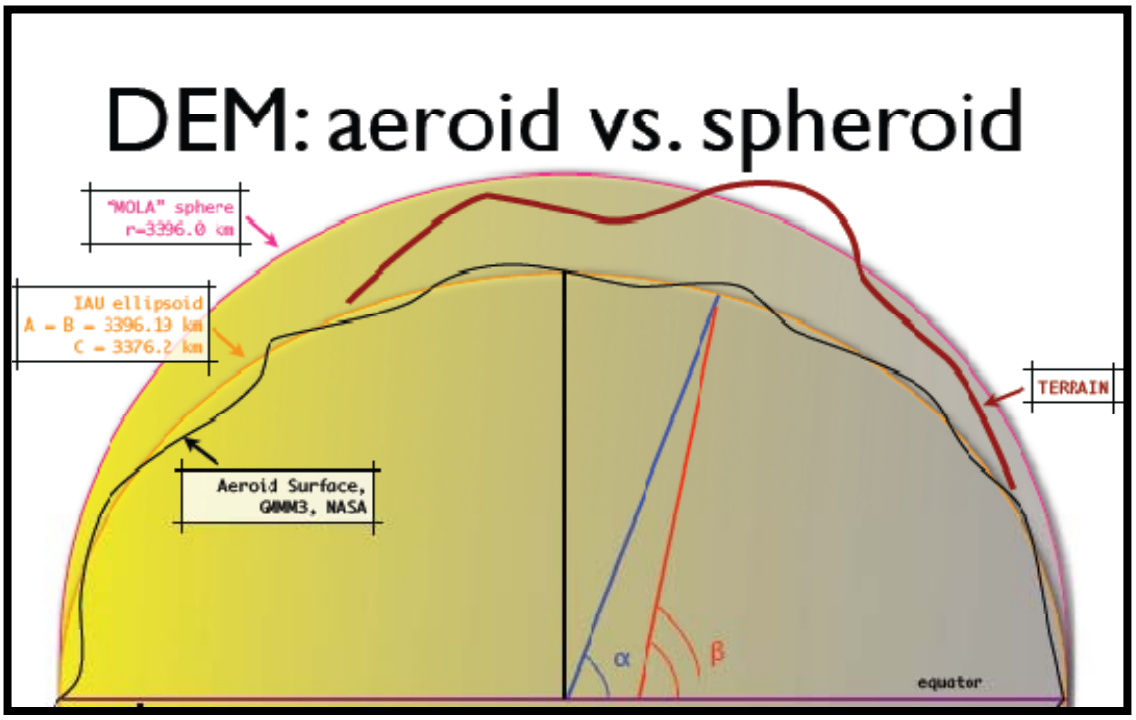

Figure 8: Image credits: Angelo Pio Rossi; HRSC Map & reference issues, Mars Express OMEGA/HRSC Data Workshop 2008

3.2.3 HRSC

The High Resolution Stereo Camera (HRSC) is an instrument onboard the Mars Express of the ESA. It was originally developed to be onboard the Mars-96 mission, which unfortunately had a launch malfunction and fell back to the Earth. The HRSC was then reselected to be part of the first mission of the ESA to Mars.
This instrument is able to make high-resolution images and to determine surface-atmosphere interactions.
This is because the Mars Express has got a strong ellipsoidal orbit (apoapsis of 10.107 km and a periapsis of 287 km). The HRSC stereo colour scanner makes stereo images, which permits a high vertical resolution of the nadir sensor of 10 m px $^{-1}$ at the periapsis (287 km). The highest image quality is attained by providing accurate spacecraft attitude and orbital data. HRSC can obtain its best resolution when the satellite is below the 500 km for more than 15 min around the pericenter. The local and regional coverage of Mars at high resolution will allow (geo)scientists to perform a detailed study of the geological stratigraphy and structures of the Martian surface.

The data is further processed at the FU Berlin and the DLR Institute of Planetary Research. For the projection of HRSC images they use a stereographical projection which is a conformal azimuthal projection (Scholten et al., 2005). With this study HRSC level-3 data is used. This data is map projected data that can directly be used in Arc GIS. Level-4 data is data that is also orthorectified. This orthorecification is part of the creation of the model and is done in the process.

3.5 Workflow:

To generate the model a base is created so other datasets can be added to it and be correlated with each other. The method used here makes use of the Mars Orbiter Laser Altimeter (MOLA) topography data. This data set has a very high resolution and is therefore ideal to refer to.
The first step in the process is to download the MOLA data and upload it in to the reservoir engineering software package `Petrel` of Schlumberger. Because the MOLA is taken as base it will not be altered after insertion in the model (figure 8).
The next step is adding the surface images and the radargrams. These can be added separately from each other, but need to be adjusted and/or modified to line up with the topography of the MOLA.

To generate the SHARAD radargrams into Petrel the images are first downloaded. The first selection can be made by selecting the radargrams that show something from the North Pole. This selection will be put in Arc GIS so SHARAD footprints can be chosen, which will be used for the model. For the model of the entire North Polar Cap, 32 SHARAD radargrams are used. The footprints are shown in figure 9 and named in appendix B1. The radargrams first have to be modified into seg-y files before they can be used in Petrel as input. This process is clearly described in Appendix C.

After the modification the SHARAD data can be used in Petrel. The objective is to line up every first reflector of each radargram with the MOLA, as they both represent the surface. Because the radargrams are still measurements in time a constant time to depth ratio is used to modify the atmospheric part of the radargrams in to depth. This is done so the distance to both the SHARAD instrument and the MOLA instrument are measured in depth and therefore should fit in the model.

The intention of this model is also to be able to drape high resolution satellite images over the surface of the NPC. These surface images will aid in the interpretation of the SHARAD data. For this study several area´s are selected, which show relevant geological area´s. The images with the highest resolution that cover these area´s are selected in Arc GIS and downloaded. To show these images in Petrel, JPG-files are made of them (see App C). In Petrel the images are given the z-values of the MOLA so a correlation with the radargrams can be made.
This process is done for several sub-areas that are described by Tanaka, 2008 (Appendix B2 and B3). These areas are chosen so it can be determined if this model is an advantage for the interpretation of the NPC.

The data is interpreted during and after the generation of the model. During the setting of the model, the data of the SHARAD have to be manually adjusted to fit correctly with the MOLA. When all the data sets line up with each other, the model can be interpreted.
Interpreting seismic data in 3D by using Petrel has already got several practical advantages. The reflectors of the surface or subsurface can be automatically traced or can be interpreted by hand. Furthermore, the crossings of these interpretations with other radargrams are visualized as well. It is therefore easier to jump from one radargram to another, to verify the interpretations made on several radargrams at one time and to create the total volume of the North Pole of Mars. When all the radargrams are interpreted an interpretation of the unit surfaces can be gridded. When done correctly the different deposition centers can be analyzed.

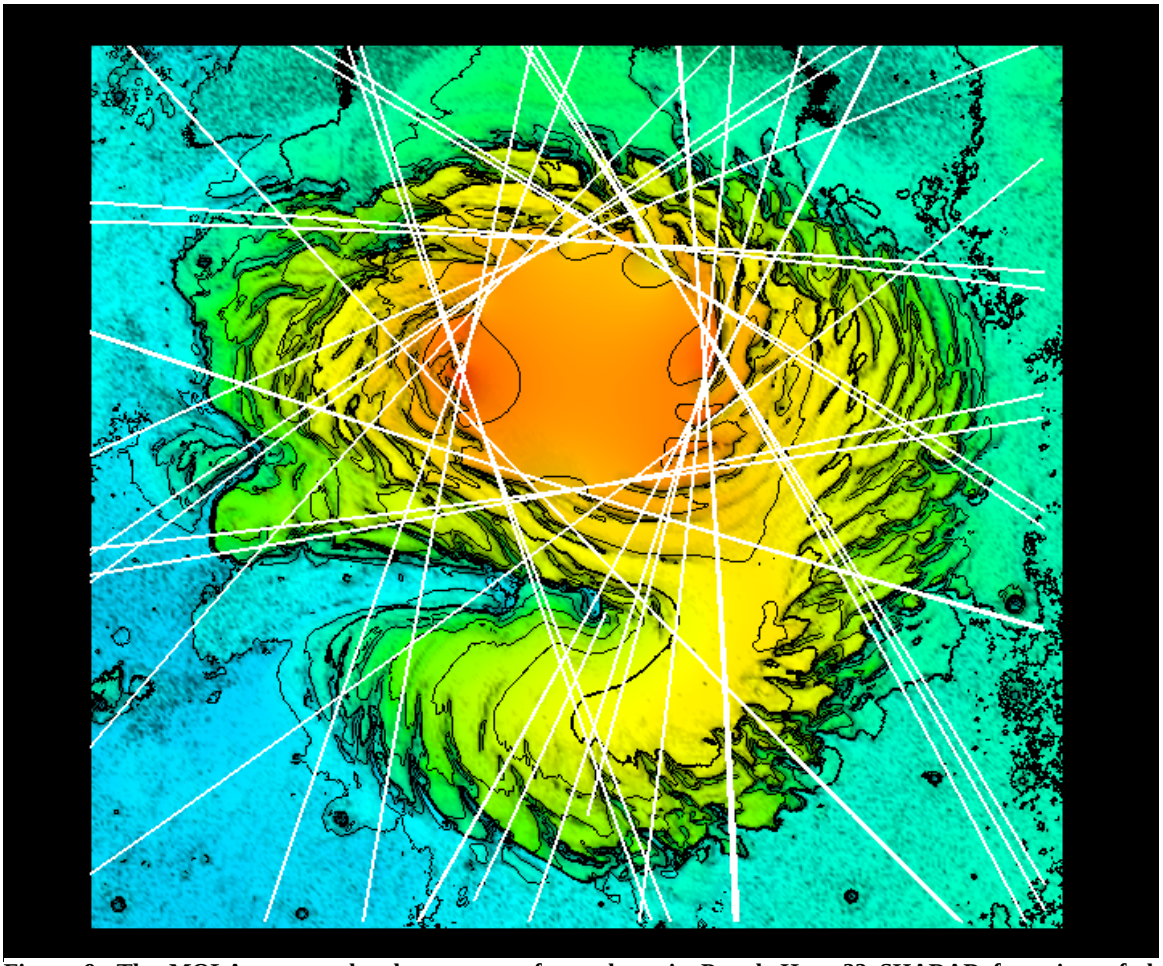

Figure 9: The MOLA topography data as seen from above in Petrel. Here 32 SHARAD footprints of the radargrams used are displayed in the figure. In Appendix B1 these footprints are named.

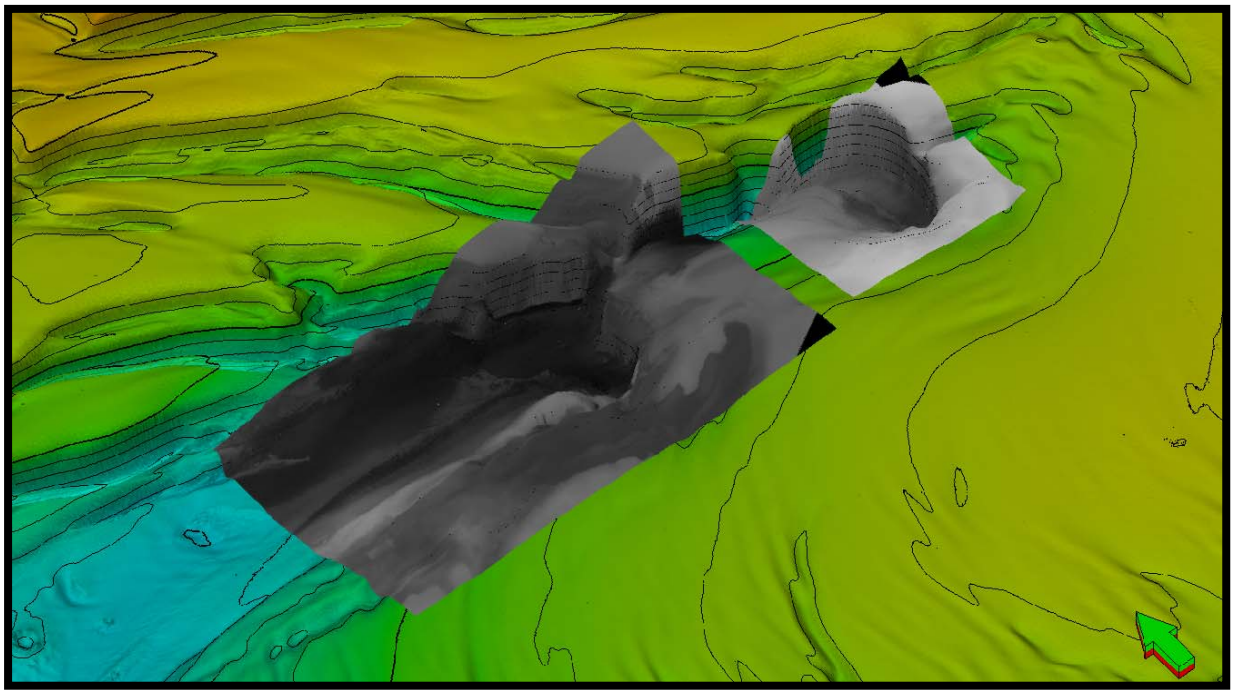

Figure 10: Two parts of HRSC surface images (f.l.t.r. H6007_0000_ND3 and 5713_0000_ND3) corresponding to two Tanaka subareas, respectively 9D and 9E drapped on the MOLA in Petrel

4. Results

In the next chapter the results of the model will be discussed. First the results of the 3D modelling phase of the MOLA and the draping of the HRSC images will be discussed. This will be followed by the results of placing the radargram in the model. Also some interpretations of the radargrams will be considered in this chapter including the resolution, clutter analyses and structural features.

4.1 3D surface model, MOLA + HRSC

The 3D model of the MOLA shows the topographic map of the NPC, measured with a laser pointer altimeter (figure 8). As said before, the MOLA is the base of this research. It is therefore assumed that the MOLA is correct. In Petrel the HRSC images are draped on the MOLA as is shown by figure 9. The sub area displayed here corresponds with subarea 9E of Tanaka *et al.* (2008), which can be used as comparison in a more detailed study of the internal structure of the NPLD. The HRSC images have no problem being projected in Petrel on the MOLA and can be used for tracking the visible layering.

4.2 Place radargram in geo-reference frame

Within Petrel the horizontal and vertical coordinates of the radargrams are checked and corrected. Some additional manipulations of the radargrams, however, do have to be made to line them up correctly in the z-direction. After this adjustment, the radargrams do fit with each other and can be correlated with the MOLA profile.

The correlation of the radargrams with the MOLA shows that the vertical coordinates also here do not correspond with each other. This was expected as they both have a different scale (figure 10). To adjust this, the radargram are stretch vertically with a factor of ~10.3 so they get the same appearance as the MOLA.

The result of this modification shows that the SHARAD radargrams, unfortunately, still do not match with the MOLA data. Figure 11 shows a close up of an offset that is still visible after stretching and shifting the radargram into an as close as possible position with the MOLA. The image also shows that the radargram bends towards the edges more strongly. This misfit can be seen in all the SHARAD images. This problem could unfortunately not been fixed during this internship.

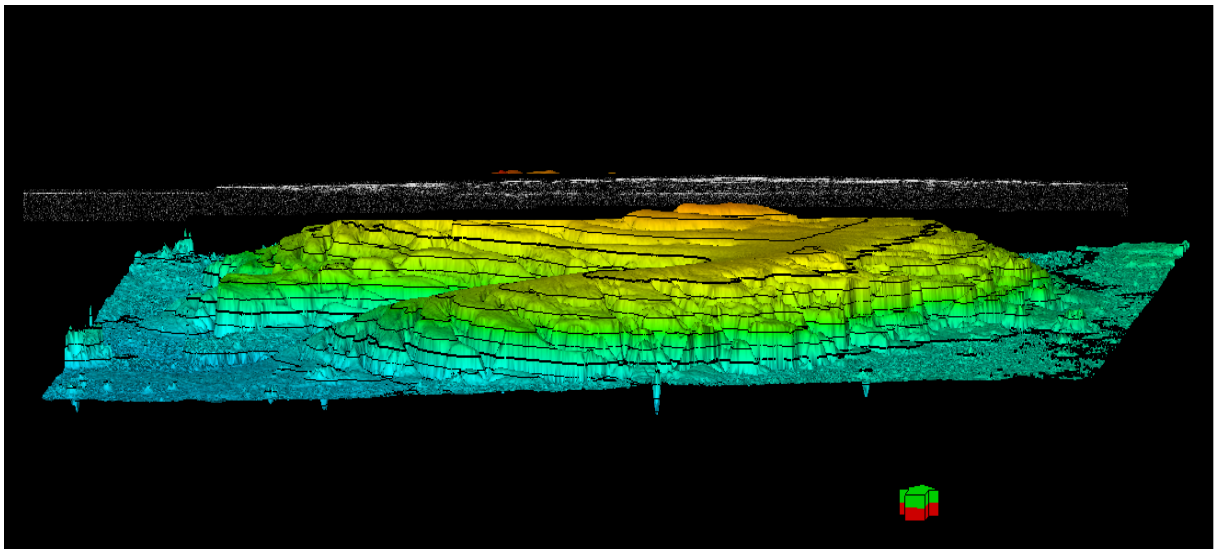

Figure 11: This figure shows the z-factor difference between the SHARAD data and the MOLA topography. By multiplying the data with a factor 10.3 the SHARAD data will obtain the right vertical setting.

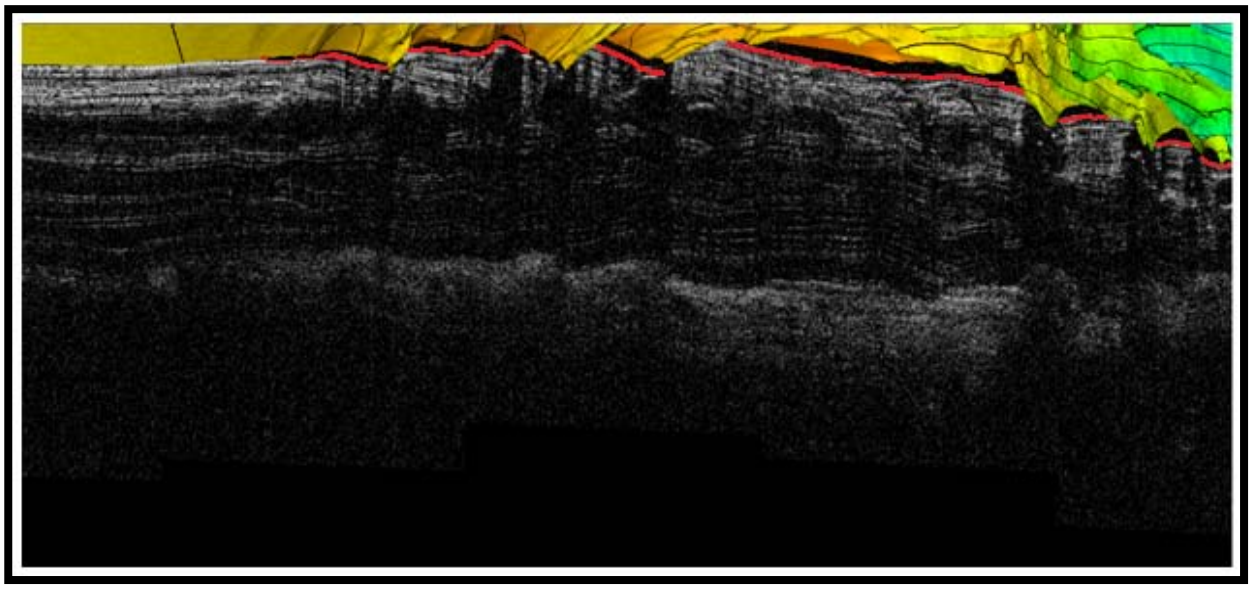

Figure 12: A clear vertical offset between SHARAD and MOLA data. The first reflector line of the SHARAD radargram has been marked with a red line. The MOLA topography flows above it.

4.3 Interpretation of radargrams

What is visible what not; limit of resolution

An interpretation, however, still could be made. Interpreting the SHARAD radargrams is part of the modelling phase in which results and modelling lay closely together.

The SHARAD data are displayed as vertical subsurface radar images, with along the axes, the distance along track versus time delay of the frequency waves. All the radargrams show multiple reflectors which characterize a change in density. It is thought that these reflector lines represent dust layers (Cutts et al., 1976; Edgett et al., 2003; Fishbaugh and Head, 2005; Milkovich and Head, 2006; Tanaka et al., 2008) or an increase in the concentration of salt.

All the radargrams have a large density of radar lines near the top, which degrades towards the bottom (figure 12). In this figure the well defined surface reflector, followed by several clear subsurface reflectors are clearly visible. This is followed by a sequence of less dense reflectors, which results in an almost entire dark ‘layer’.

This sequence, of a very dense layer of reflectors followed by a dark layer of not much reflectors, can be seen four times in total in this radargram. To illustrate this sequence of layers, the boundaries interpreted seen in figure 12 have been marked and shown in figure 13. The interpretations are further discussed in the next section 4.4.3.

The result of the decrease in energy of the radar with depth is also visible in these figures. To illustrate this, the centre and the left side of the radargram are compared. The reflector intensity in the centre of the image shows a clear decrease, which is the result of a loss of energy. The decrease in energy causes that the lower layers are not clearly visible. Seen in the radargrams at the edges of the ice cap the radar energy can reach the lower layers, so their structure can be made visible.

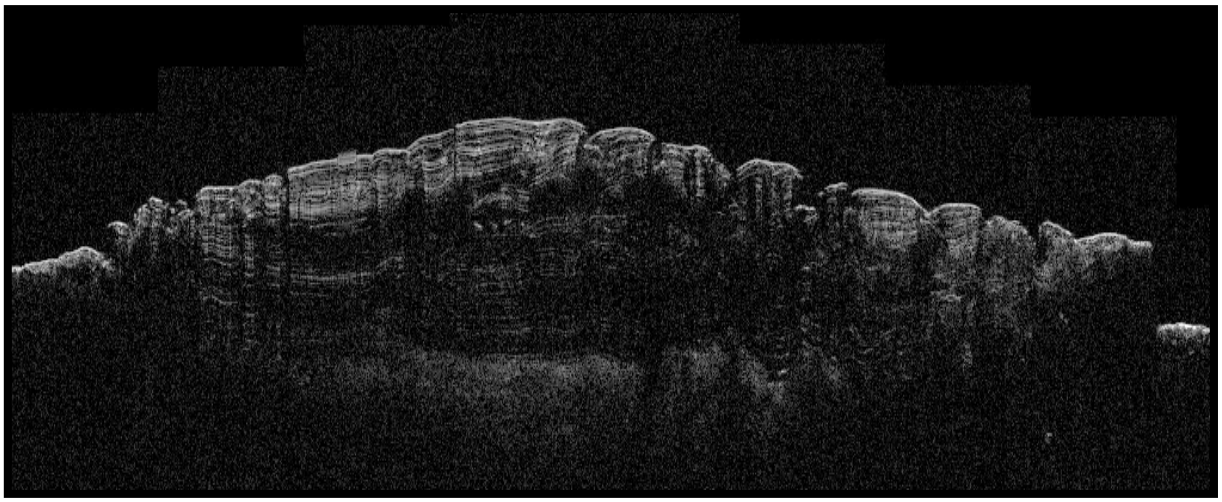

Figure 12: Vertical scale in time delay (r_0478602_001_ss11_700_a_1). Because the radargrams are not yet scaled from time to depth the figure does not shows a scale.

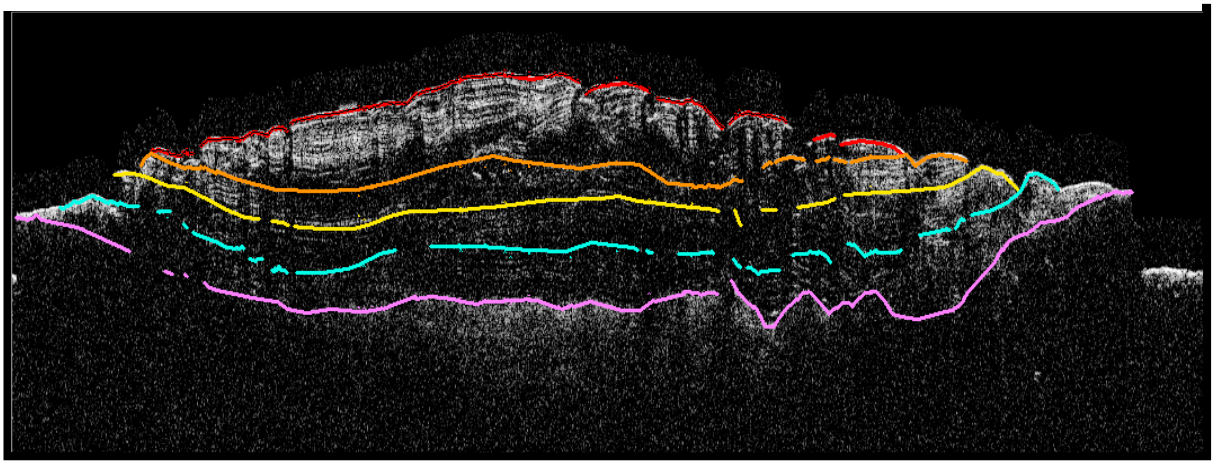

Figure 13: Vertical scale in time delay (r_0478602_001_ss11_700_a_1)

The interpreted radargrams are combined together to create a three dimensional model of the NPC. The interpreted surface can be seen in figure 14. In this figure the topography of the MOLA is also shown for comparison. One clear difference between the MOLA and the model is the resolution of the surface. The MOLA surface shows clear and sharp topographic changes such as the characteristic troughs of the North Pole. The NP-model does not show this and only shows a smooth curved surface. This can be explained by the fact that this surface has been buildup out of just 32 radargrams. More interpreted radargrams are needed to make a more accurate surface interpretation.
The straight lines, which run over the model, can be explained as artifacts in the surface editing of the program and represent interpreted radargrams.

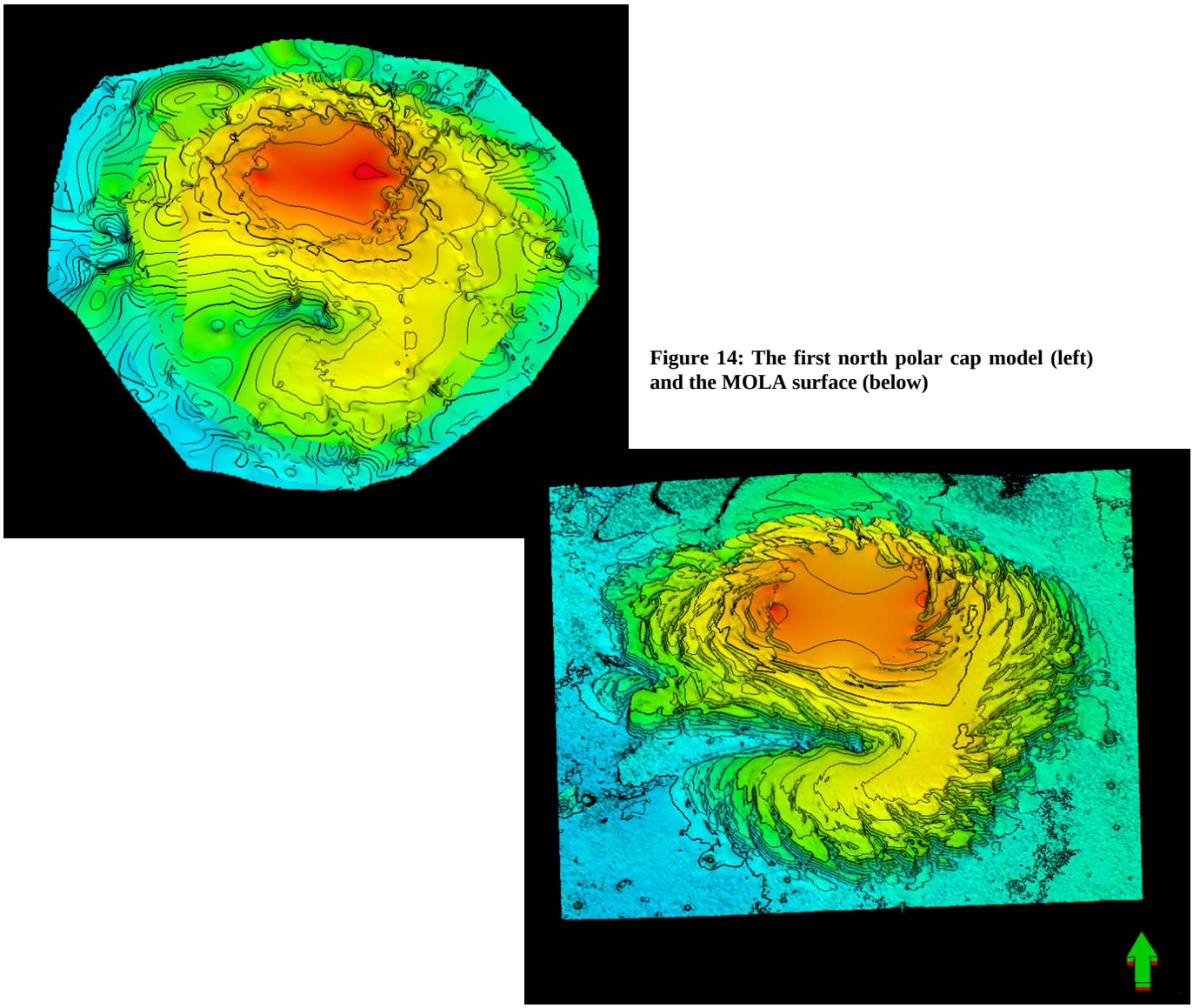

Figure 14: The first north polar cap model (left) and the MOLA surface (below)

4.4 Geology

4.4.1 Faults

The interpretation of the radargrams of the NP-model seems to give evidence for faults near the trough system of the ice cap (figure 15). The radar image show a lower continuation of the layers and units at the places where troughs can be founds. The most important reason for the assumption that there could be a listric fault system is the fact that the units seem to keep their size until it runs horizontal near one of the two blue boundaries.

Fault structures are not a new feature that could occur in the ice cap of Mars. Milkovich and Head (2006) show clear evidence of faulting on surface images of the NPC. These images show low angle reverse faults and normal faults. Also Tanaka *et al.* (2008) finds evidence of faults, but at a smaller scale. They stated that these minor faults are probably produced by sedimentary loading, deposition of material or surface erosion, which causes compaction and failure.

4.4.2 Spiral Troughs

The spiral trough system is an intriguing feature of the Polar Cap that gives the North Pole its structure. They wave out counter clockwise while cutting through the NPLD exposing equator facing dusty ice layers. These scarps are also long suggested to be the source for the dune systems near the ice cap (Howard et al., 1982; Clifford, 1987; Fisher, 1993; Edgett et al., 2003).

Theories about the formation of the troughs in the ice cap have come up throughout the years, mainly stating that some kind of ablation has formed the troughs. This ablation could be in the form of wind erosion (Howard et al., 1982; Edgett et al., 2003), ice flow (Fisher, 1993; Winebrenner et al., 2008), sublimation (Howard, 1978) or faulting (Ng and Zuber, 2006; Zeng et al., 2007).

The model aids in the process of finding the cause of these troughs. It is believed that faults can be seen on the radargrams at the places where troughs are visible on the surface images. This model therefore also supports a fault history for the trough system.

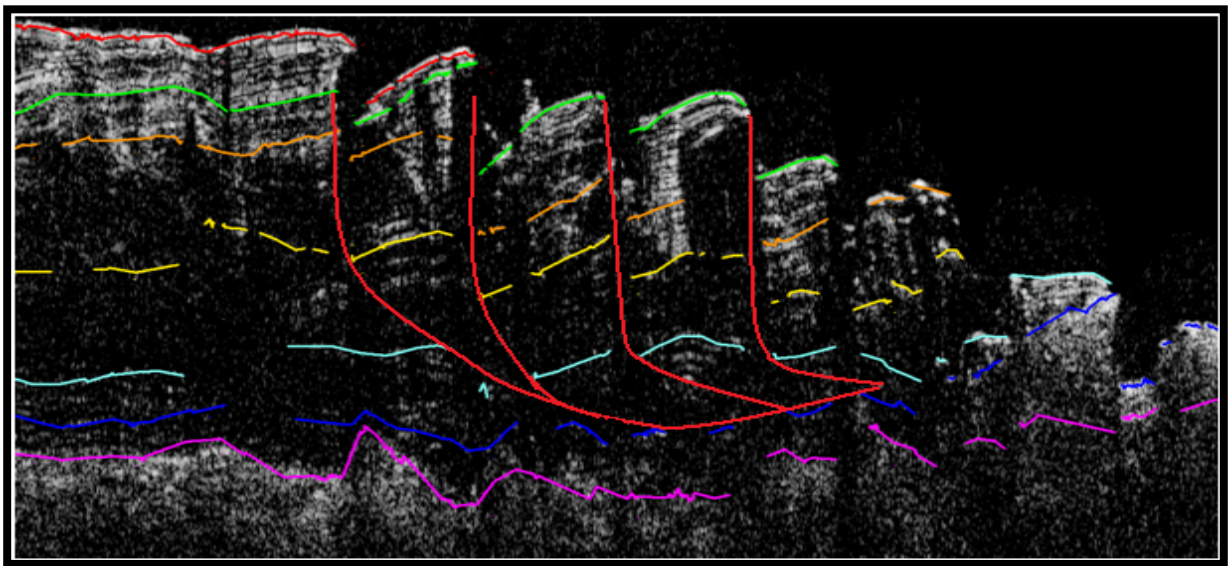

Figure 15: The lystric faults are represented here in red. They seem to be near-vertical faults, but this effect is due to vertical over excaturation, SHARAD radargram 23515_r_0557002_001

4.4.3 Layering

The interpretation of the radargram also shows clear lines throughout the entire NPC of Mars. These statements could not yet be made with the surface images and shows the advantage of the radargrams. Four major layer units can be identified when studying the images as represented in figure 13. Per layer, they all seem to show a dense package of reflectors in the upper part of the unit and a less dense part of reflectors in the lower part. As this sequence repeats itself various scientists have explained this as being the result of a cyclic event due to the obliquity and eccentricity of Mars (Laskar et al., 2002; Levrard et al., 2007; Perron and Huybers, 2009). A better age determination of the ice cap will therefore be obtained when the layers are closely determined.

Layers can be seen on the HRSC surface images and on the SHARAD radargrams which are not smaller than ~100 meters. With this resolution internal structures can be seen that cross other layers or are cut off by other layers (figure 16a and 16b). The structure suggests that erosional features have altered the layering. The structure seems to imply that angular unconformities characterize the ice and dust deposition (Tanaka, 2005; Fishbaugh and Hvidberg, 2006; Milkovich and Head, 2006).

As this feature can only be seen in the upper part of the ice cap, nothing can be said if this structure continues with depth.

4.4.4 Link between SHARAD and HRSC

Linking the SHARAD data with the HRSC images also shows a clear misfit. As the surface images represent smaller areas the errors can even be seen more clearly (figure 17). The HRSC images are projected on the MOLA, so this result was not unexpected.

Trying to correlate layers found on the SHARAD radargrams with the layers found on the HRSC images is hard to carry out. The layers are not connected due to the misfit and thus need to be compared another way. A solution is to describe the layers individually, by describing their characteristics and sequence. If this correlates on both the HRSC as the SHARAD images the assumption can be made that they belong together and a fit can be made.

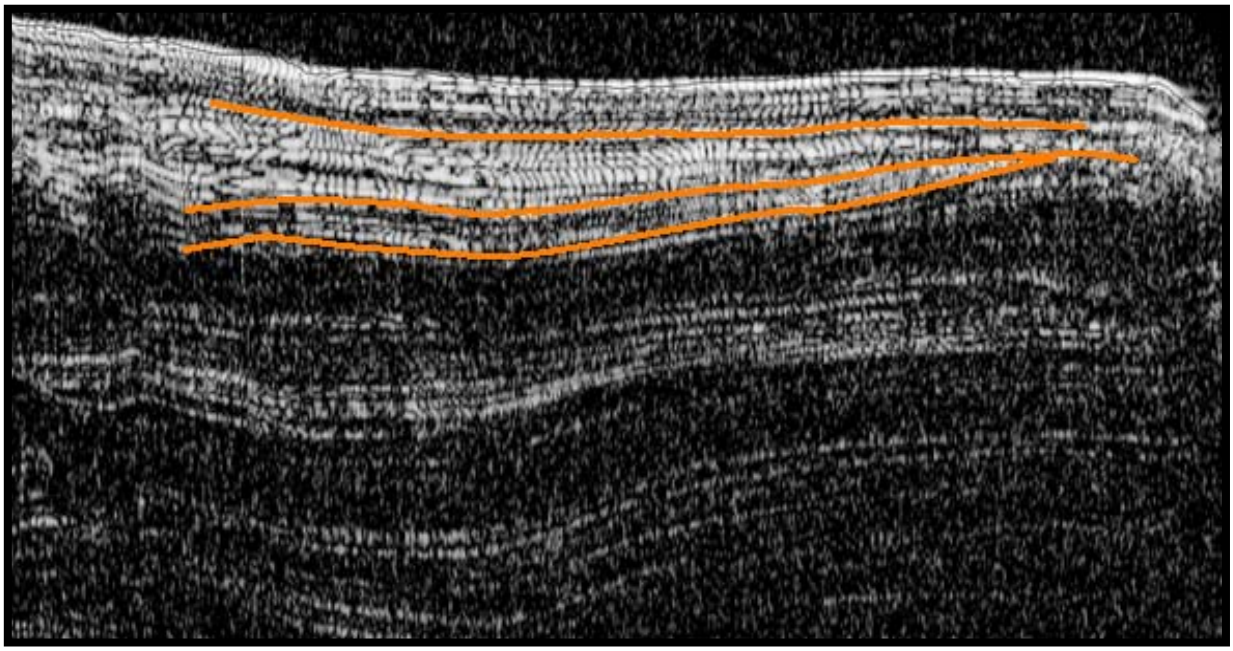

Figure 16a: Example of layers that seem to cut each other of in the about unit layer. 273908_r_0614102_001

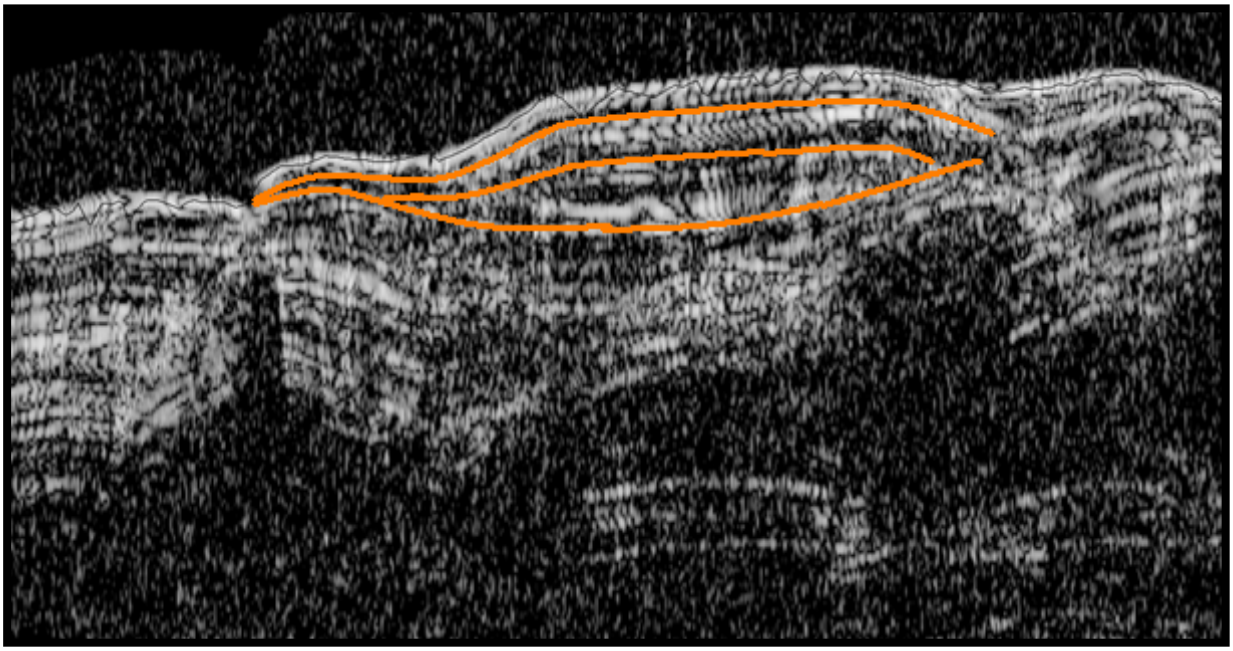

Figure 16b: Another example of layers that seem to cut each other of in the about unit layer 245458_r_0444101_001

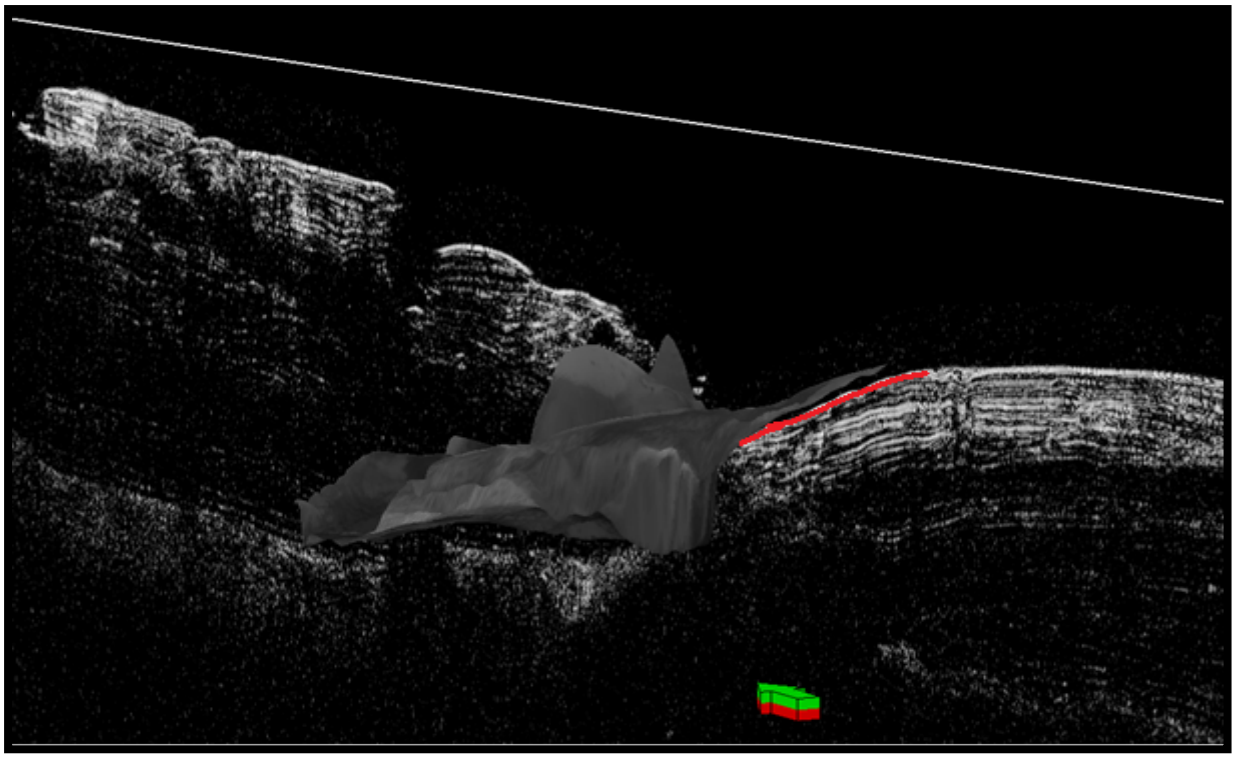

Figure 17: The link between SHARAD and HRSC surface images. The red line represents the surface of the north polar cap shown by SHARAD. A misfit is shown between the surface image of a subarea and the radargram.

5. Conclusion/ Recommendations

5.1 Goal

The goal of this research is to create a 3D model of the Northern Polar Cap of Mars by using SHARAD radargrams and HRSC surface images. The method used in this research, uses the MOLA as a reference frame, because of its high resolution.
The surface images were draped over the MOLA and the SHARAD radargrams were inserted to correlate it with the geology and morphology seen on the surface images. Unfortunately, as the results show, this goal can not be met as the radargrams do not fit with the MOLA.

5.2 Problem cause

Possible reasons why this offset occurs can be the result of several data processes:

-*The different orbits of the 2 satellites.*
Although it is stated by the group of the SHARAD and the MOLA the data is processed for this, it is still possible that the resulting two data sets of the MOLA and from the SHARAD do not fit for the same projection.

-*The error range of the SHARAD instrument.*
It is very well possible that the rough terrain caused by the trough-systems increase the uncertainty of the data sent back. Remember the error range for most Martian surfaces was about 3-6 km for cross-track and 0.3-1 km for along-track. This is probably larger for this rough, quickly changing, terrain and therefore could cause the misfit with the MOLA.

-*Our own processing during the modelling.*
This is, however, thought to be unlikely, because the data has hardly been altered during the process of creating SEQ-Y's. The data downloaded has almost directly been used and put in the modelling program. Therefore no flaws are expected here.

-*Time depth conversion*
The time to depth conversion that has been applied to the SHARAD data can also be a possible cause of the offset found in the model. In this model only the atmosphere has been converted to depth. One of the problems that can occur with this time depth conversion is a wrong dielectric constant for the atmosphere. The atmosphere is a continually changing factor and therefore can cause different measurements. Determining the time correctly when the radar signals of the SHARAD enter the atmosphere of Mars and thus determining the time between the entering of the atmosphere and hitting the surface, also have to be taken into account.

-*Ionosphere effect*
The upper layer of the atmosphere, the ionosphere, should also be taken into account as a possible influence on the miss fit. The radiowaves that come through the ionosphere lose their energy and therefore can influence the data that is coming back to the instrument.

5.3 Other modelling reports

Previous modelling of the NP has been done by Putzig et al. (2009). In this report the North Pole is constructed out of 358 radargrams and concentrates its study on the subsurface of the ice cap. The model of Putzig et al. does not have a reference frame with the MOLA data, as they do not compare it with surface images. The SHARAD images are only correlated with each other, which results in a well interpreted model.
No other SHARAD modeling reports have been written, which is unfortunate as a three dimensional view of the radar images can lead to a better interpretation of the North Polar Cap.

5.4 Scientific work with the results

5.4.1 Structural interpretation of radargrams.

Scientifically the model can still be used to explore the continuity of the layers and their characteristics. Separate characterizing of the layers on both the radargrams and the surface images can eventually be coupled by analyzing both stratigraphic columns.

5.4.2 Obtaining a 3D model (incl. MOLA fit)

Other or extra steps have to be taken to produce a good model as the method used in this research did not achieve its goal. Geo-referencing can be a attempted to aid in the modelling process. The extra step in the modelling phase would be to geo-reference the first reflector of the SHARAD radargrams with the MOLA surface in ArcGIS. After this manipulation the data can be transformed into seg-y data and can be used in Petrel. It is expected that the SHARAD data and MOLA will show a fit. This solution, however, includes that all radargrams have be manually geo-referenced and is therefore time consuming.

6. Acknowledgements

I would like to thank Jelmer H.P. Oosthoek, Marco H.P. Kleuskens and Tanja E. Zegers for supporting me during the entire research period and stimulating me with all kinds of thoughts and inspiration. I also would like to give special thanks to Edward C. King of the Britisch Antartic Survey and Jack W. Holt and Marcel Bakker who gave personal help and enthusiasm within this research.

7. Appendix

A: List of used Python scripts

A small description of the Python scripts can be found in Appendix C. Here they are recorded in the workflow for the SHARAD and HRSC data.
For a full description and information there is referred to Oosthoek, J.H.P.

-SHARAD_csv_addMOLA.py
-SHARAD_jpgdownload.py
-SHARAD_index2shapefile_checked.py

-The GreatCircle class, vinc_dist def and vinc_pt def mentioned in this script can be found at: http://www.koders.com/python/fid0A930D7924AE856342437CA1F5A9A3EC0CAEACE2.aspx?s=coastline.

-SHARAD_datadownload.py
-SHARAD_dat2asc.py
-SHARAD_csv_addTIME.py
-Contents Mars NP Stereographic Sphere.prj:
-Contents BSQ2JP2.bat:

B: SHARAD footprints used for modeling

B1

SHARAD footprints used for modeling the NP-model	
r_0557002_001_ss11_700	r_0478402_001_ss11_700
r_0580702_001_ss05_700	r_0444101_001_ss19_700
r_0496302_001_ss05_700	r_0765803_001_ss05_700
r_0856202_001_ss05_700	r_0488901_001_ss19_700
r_0434202_001_ss05_700	r_0498102_001_ss05_700
r_0699202_001_ss11_700	r_0614102_001_ss11_700
r_0472302_001_ss11_700	r_0557402_001_ss11_700
r_0522402_001_ss11_700	r_0893602_001_ss05_700
r_0699002_001_ss11_700	r_0563902_001_ss11_700
r_0478802_001_ss11_700	r_0735302_001_ss11_700
r_0886102_001_ss11_700	r_1042502_001_ss05_700
r_0742402_001_ss11_700	r_0656102_001_ss11_700
r_0478602_001_ss11_700	r_0521602_001_ss11_700
r_0429802_001_ss11_700	r_0429202_001_ss11_700
r_0656503_001_ss11_700	r_0479302_001_ss11_700
r_0698602_001_ss11_700	

B2

SHARAD footprints used for modeling the sub areas (area 9e)	
r_0459101_001_ss19_700	r_0420401_001_ss19_700
r_0438001_001_ss19_700	r_0342601_001_ss19_700
r_0416901_001_ss19_700	r_0434901_001_ss19_700
r_0339101_001_ss19_700	r_0336001_001_ss19_700
r_0176902_004_ss19_700	r_0619501_001_ss19_700
r_0176902_003_ss19_700	r_0449401_001_ss19_700
r_0439301_001_ss19_700	r_0350501_001_ss19_700

r_0588301_001_ss19_700	r_0598401_001_ss19_700
r_0489401_001_ss19_700	r_0442801_001_ss19_700
r_0482801_001_ss19_700	r_0421701_001_ss19_700
r_0440601_001_ss19_700	r_0343901_001_ss19_700
r_0341701_001_ss19_700	r_0436201_001_ss19_700
r_0589601_001_ss19_700	r_0492901_001_ss19_700
r_0490701_001_ss19_700	r_0620801_001_ss19_700
r_0526301_001_ss19_700	r_0599701_001_ss19_700
r_0505201_001_ss19_700	r_0614201_001_ss19_700
r_0484101_001_ss19_700	r_0444101_001_ss19_700
r_0519701_001_ss19_700	r_0423001_001_ss19_700
r_0341301_001_ss19_700	r_0593101_001_ss19_700
r_0448101_001_ss19_700	r_0458601_001_ss19_700
r_0441501_001_ss19_700	r_0437501_001_ss19_700

B3

SHARAD footprints used for modeling the sub areas (area 2)	
r_0245801_002_ss11_700	r_0177901_002_ss19_700
r_0306402_002_ss05_700	r_0284702_002_ss05_700
r_0306402_001_ss05_700	r_0293902_004_ss11_700
r_0285302_001_ss05_700	r_0293902_003_ss11_700
r_0264202_002_ss05_700	r_0251701_003_ss11_700
r_0264202_001_ss05_700	r_0337401_001_ss19_700
r_0202201_004_ss19_700	r_0196301_006_ss19_700
r_0252301_002_ss11_700	r_0444201_001_ss19_700
r_0307602_002_ss05_700	r_0423101_001_ss19_700
r_0307602_001_ss05_700	r_0458701_001_ss19_700
r_0442101_001_ss19_700	r_0437601_001_ss19_700
r_0286502_001_ss05_700	r_0416501_001_ss19_700
r_0265402_001_ss05_700	r_0338701_001_ss19_700
r_0343201_001_ss19_700	r_0409901_001_ss19_700
r_0435501_001_ss19_700	r_0445501_001_ss19_700
r_0336602_001_ss19_700	r_0424401_001_ss19_700
r_0351102_001_ss19_700	r_0438901_001_ss19_700
r_0172701_002_ss19_700	r_0417801_001_ss19_700
r_0203001_006_ss19_700	r_0340001_001_ss19_700
r_0253101_003_ss11_700	

C: Processing the data into usable files for Petrel.

Generating SHARAD radargrams for Petrel.

Creating SHARAD footprints for Arc-GIS:

1. All the data from the MRO, SHAllow RADar has been made available by NASA on *http://pds-geosciences.wustl.edu/missions/mro/sharad.htm*. By following 'RDR' "Reduced Data Records" > 'Index' all the SHARAD data that has been released until then, can be obtained. By using a Python script (see *SHARAD_index2shapefile.py*) the 'Index'-dataset will be automatically downloaded and converted into a useable **ESRI shapefile**.

2. Because this project has its study area concentrated at the North Pole of Mars, shapefiles of the North Pole with a latitude >75^{o} were created.

3. The locations of the **.DAT RDR** files and the **.JPG browse** images were added in the Attribute Table to make the footprints easier in use.

View in Arc-GIS

4. By loading the **ESRI shapefiles** into Arc-GIS the DataFrame needs to be set to NP Stereographic Projection to generate a view centered on the North Pole.

5. For a better orientation for these lines the data from the Mars Orbital Laser Altimeter (MOLA) is also downloaded and inserted in Arc-GIS. This can be downloaded from: *http://webgis.wr.usgs.gov* > Download >'MOLA DEM's GIS-ready downloads' > 'polar' directory. This directory gives three scales: 128, 256 and 512 pixels per degree, which represents 460,4 m/pixel, 230,2 m/pixel and 115,1 m/pixel respectively. The highest resolution of 512 pixels per degree only shows the polar area, which is large enough for this project and is therefore also the image used as a reference.

Selecting the data

6. All or a subset of the SHARAD data can now be selected in Arc-GIS. By exporting the Attribute Table of the data to a **.DBF-file** the **JPG-links** can be put into an **ACII.txt-file.**

7. This newly made **.TXT-file** will be used as input in a Python script (see *Sharad_jpgdownload.py*) and will download all the **.JPG-files.**

8. All the **JPG-**images are then visually inspected and checked on their relevance. From the relevant images a new shapefile is created containing the relevant footprints. This is done with the Python-script *SHARAD_index2shapefile_checked.py*.

9. From the selected **JPG-files,** the **.DAT RDR**-data and the accompanying **.lbl header-files** were downloaded using *SHARAD_datadownload.py*. This downloads the relevant raw data, which is needed to create **SEG-Y data files** in a later stage.

Creating SHARAD SEG-Y data for Petrel

10. To generate SHARAD input files for Petrel, **SHARAD_dat2asc.py** is used. The **SHARAD_dat2asc.py** uses the area coordinates of the studied area (in the **.INI**) and the **DAT RDR**-data as input and creates a **.ASC**–file, which contains the radargram information and a **.CSV**-file, which contains the spatial footprint information.

11. The output is then used as input for **SHARAD2seqy.java** to generate the **SEG-Y** files. These **SEG-Y** files can be used for Petrel.

Generating HRSC-images as input for Petrel

How to generate drape-over pictures for Petrel:

1. In ArcGIS the Tanaka.PNG (Fig 4) is opened. This figure will be used to choose the specific sub-areas of which the surface images are used for detailed study.

2. On top of the Tanaka image the HRSC footprints are displayed and the area that is wanted for study is selected. **Note:** Images of high quality (high resolution) are preferred in this detailed study.

3. By using FileZilla the zip-files belonging to these pictures can be downloaded. For this, the ESA Planetary Science Archive FTP site is used: ftp://psa.esac.esa.int/pub/mirror/MARS-EXPRESS/HRSC/MEX-M-HRSC-5-REFDR-MAPPROJECTED-V2.0/DATA/
The **0000-** or **0001-ND3.IMG-file** in the right column are used for this study, as these give the highest resolution.

4. From this point two ways can be chosen of creating a JP2000 and a JPG. One method is by using ArcGIS and the other is by using GDAL (http://fwtools.maptools.org/). Both methods are used and will be explained.

When using ArcGIS:

5.1.1 When using ArcGIS method the downloaded **ND3.IMG-file**, will be used as input for the HRSC application. This application will generate a **BSQ-file**. The executable itself can be downloaded from *http://arcscripts.esri.com/details.asp?dbid=15566* (32bit PC only). The **BSQ-file** can then be imported in ArcGIS.

5.1.2 In ArcGIS the images are checked if the pictures are geo-referenced well enough. After this a **JP2-file** can then be generated. This can be done by exporting the data. The **JP2-file** type will, eventually, be the automatic input of ArcGIS, which is much smaller in size and has been transformed from a sinusoidal projection to an on-the-fly projected image. For this, one has to make sure that the Spatial Reference is put on 'Data Frame' and the Extent on 'Raster Dataset' (see figure C1).

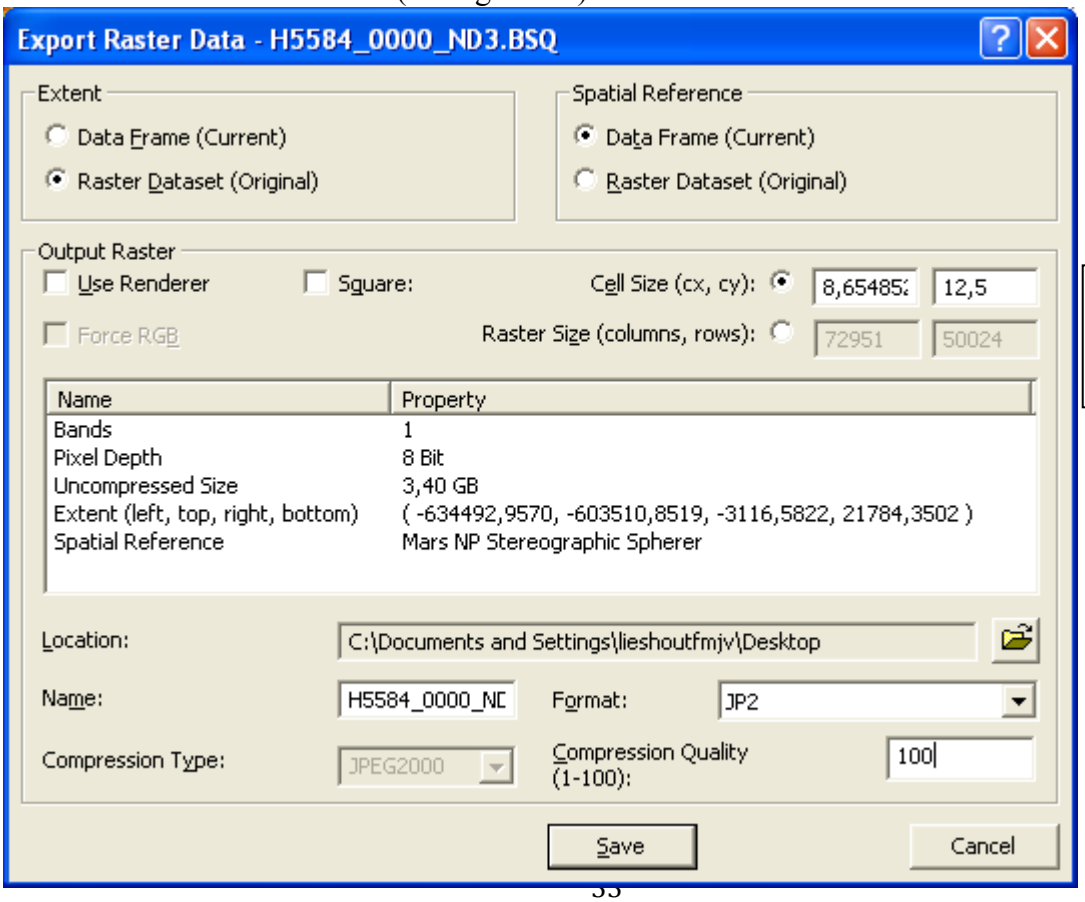

Fig C1: Generating a JP2-file in ArcGIS

5.1.3 When the **JP2** has been made, a **JPG-file** can be made of it. Here only the section of the image, which is being studied, needs to be shown in the screen. Then again export it. But this time choose Data Frame for both settings and for Format choose **JPG.** This process will generate a **JPG input-file**, which can be used in Petrel.

When using GDal:

5.2.1 When using GDal we can use the original **BSQ-file** and run the GDal program through **BSQ2JP2.py**. This will generate a **JP2-file**, which then can be used as input for ArcGIS to generate a **JPG-file** in the same way as already mentioned above (5.1.3). The **IGE-** and **IMG-file** can be deleted after the **JP2-file** has been made.

Note: In the **BSQ2JP2.py** the Spatial Reference is automatically set to Mars NP Stereographic Sphere. Also note that for every new **BSQ-file** the application needs to be updated for the specific image.

Input in Petrel:

6. To use the images in Petrel the x- and y-extent of the image need to be given, to drape it over the MOLA-data. Two of the four coordinates that are needed, can be found in the **HDR**-file. The other two coordinates can be calculated using the image width and height and the m/pixel resolution also found in the **HDR**-file.

Note: When using surface images in Petrel to visualize the topography, make sure the Petrel license has got the 'Surface Imaging' enabled.

Fig C2: Generating a surface of the JPG-file

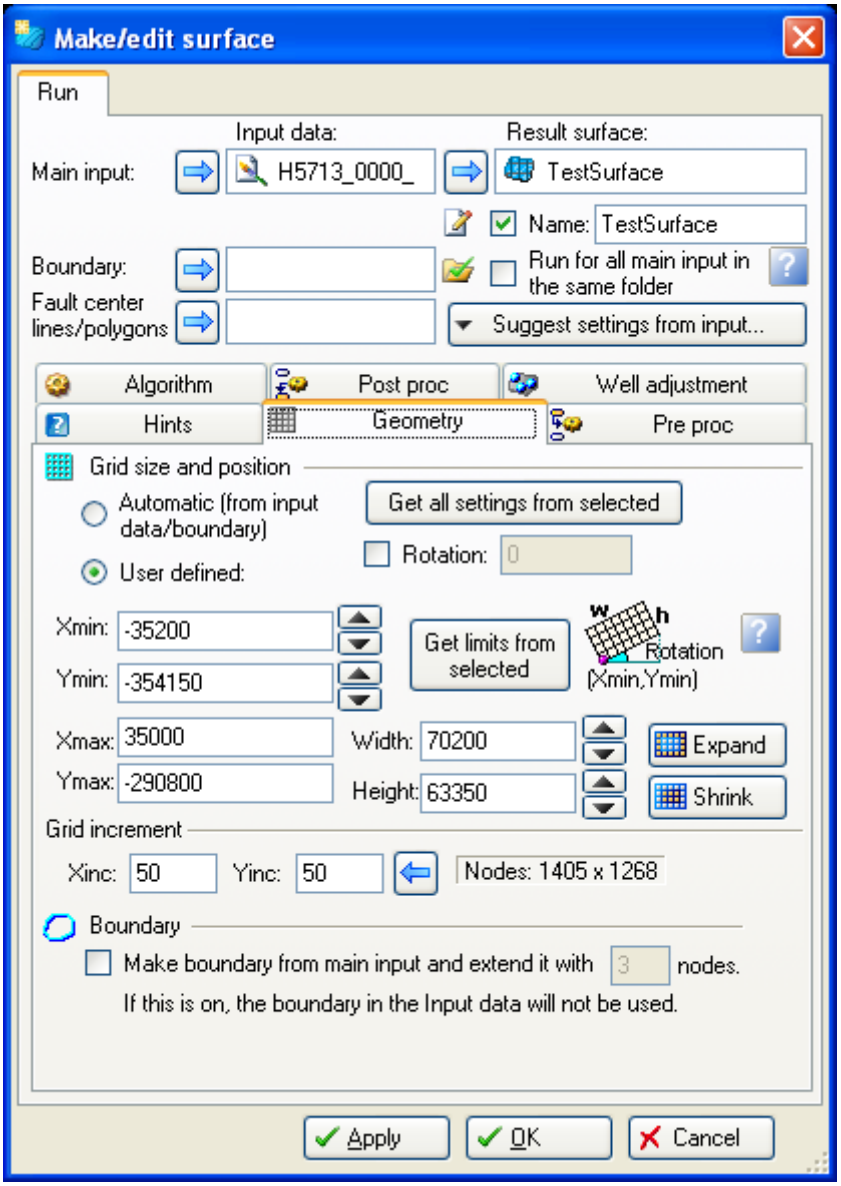

To import the image in Petrel with the JPG-file, do the following:

7. To import the image and give it the right z-value several steps have to be taken. First go to Processes>Utilities>Make/edit surface. As main input enter "*The Image Name*". At the tab 'Geometry' enable '*User defined'* and click on '*Get limits from selected'* (fig.C2). At Tab 'Algorithm' choose from the pull-down menu Method>Surface resampling and then click Apply. The new surface is generated.

8. Go to Operations>Arithmetic operations by clicking on the new surface and click on '*Z = Surface (x,y)*'. Use the **NP.dat** as input data and run the operation. The new surface will now get the same z-values as **NP.dat**.

9. For the final step go from the Tab '*Style'* to the Tab '*Solid'* and choose Color>Textured>"*The Image Name"*, see figure C3. The new surface now will adapt the color features of the **Jpg-file.**

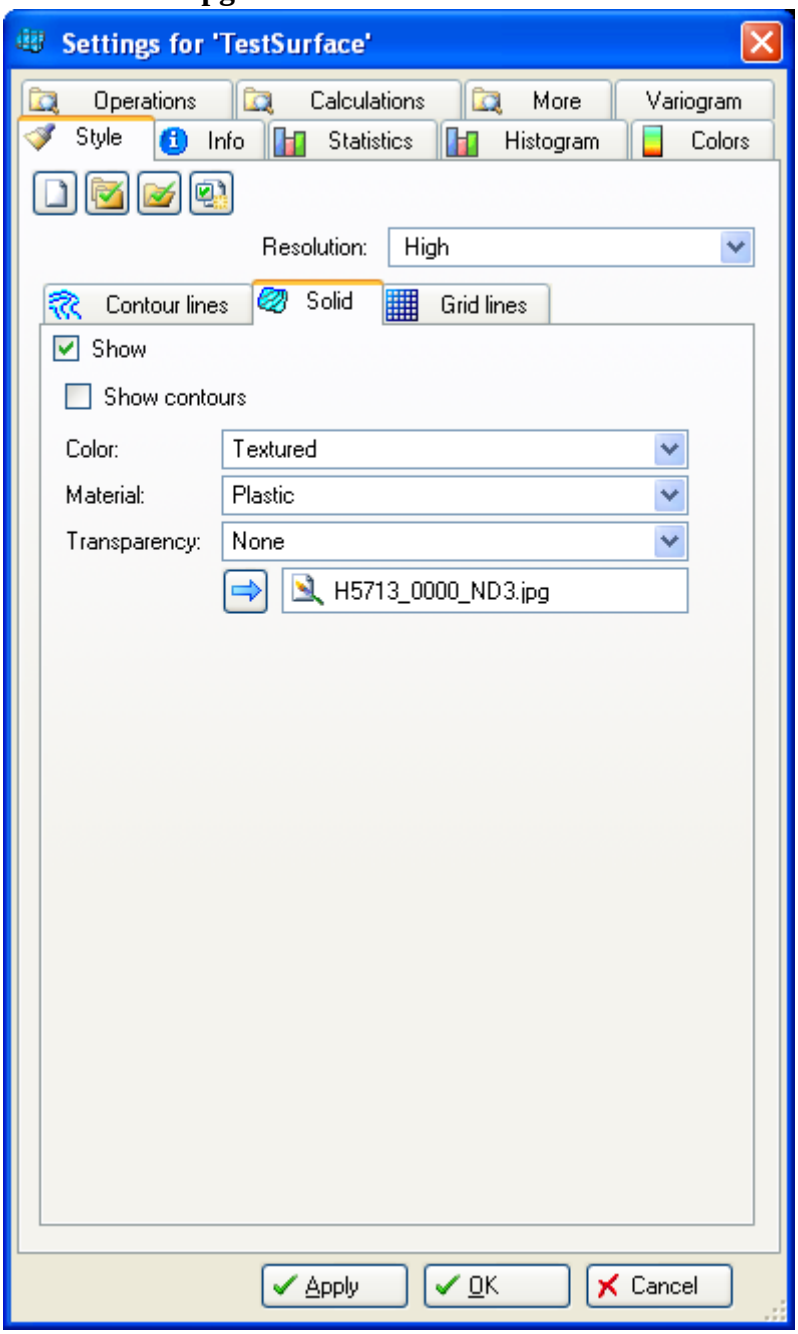

Fig C3: Setting the imaging of the surface

After inserting the **SEQ-Y** files in Petrel all the files separately have to be adjusted manually to line up with the MOLA topography. This includes changing the sample interval factor and the shifting the whole line. Only vertical adjustment and no horizontal adjustments can be made with the radargrams.

8. References

Abshire, J.B., Sun, X.L., and Afzal, R.S., 2000, Mars Orbiter Laser Altimeter: Receiver model and performance analysis: Applied Optics, v. 39, p. 2449-2460.

Anguita, F., Babin, R., Benito, G.*, et al.*, 2000, Chasma Australe, Mars: Structural Framework for a Catastrophic Outflow Origin: Icarus, v. 144, p. 302-312.

Bass, D.S., Herkenhoff, K.E., and Paige, D.A., 2000, Variability of Mars' North Polar Water Ice Cap: I. Analysis of Mariner 9 and Viking Orbiter Imaging Data: Icarus, v. 144, p. 382-396.

Benito, G., Mediavilla, F., Fernandez, M.*, et al.*, 1997, Chasma Boreale, Mars: A sapping and outflow channel with a Tectonothermal origin: Icarus, v. 129, p. 528-538.

Boisson, J., Heggy, E., Clifford, S.M.*, et al.*, 2009, Sounding the subsurface of Athabasca Valles using MARSIS radar data: Exploring the volcanic and fluvial hypotheses for the origin of the rafted plate terrain: J. Geophys. Res., v. 114.

Byrne, S., 2009, The Polar Deposits of Mars: Annual Reviews of Earth and Planetary Sciences v. 37, p. 535-60.

Clifford, S.M., 1987, Polar Melting on Mars: J. Geophys. Res., v. 92, p. 9135-9152.

Clifford, S.M., 1993, A Model for the Hydrologic and Climatic Behavior of Water on Mars: J. Geophys. Res., v. 98, p. 10,973-11,016.

Cutts, J.A., Blasius, K.R., Briggs, G.A.*, et al.*, 1976, North Polar Region of Mars: Imaging Results from Viking 2: Science, v. 194, p. 1329-1337.

Edgett, K.S., Williams, R.M.E., Malin, M.C.*, et al.*, 2003, Mars landscape evolution: influence of stratigraphy on geomorphology in the north polar region: Geomorphology, v. 52, p. 289-297.

Fishbaugh, K.E., Byrne, S., Herkenhoff, K.E.*, et al.*, 2009, Evaluating the meaning of "layer" in the martian north polar layered deposits and the impact on the climate connection: Icarus, v. In Press, Corrected Proof.

Fishbaugh, K.E., and Head, J.W., 2000, North polar region of Mars: Topography of circumpolar deposits from Mars Orbiter Laser Altimeter (MOLA) data and evidence for asymmetric retreat of the polar cap: Journal of Geophysical Research-Planets, v. 105, p. 22455-22486.

Fishbaugh, K.E., and Head, J.W., 2005, Origin and characteristics of the Mars north polar basal unit and implications for polar geologic history: Icarus, v. 174, p. 444-474.

Fishbaugh, K.E., and Head, J.W., III, 2002, Chasma Boreale, Mars: Topographic characterization from Mars Orbiter Laser Altimeter data and implications for mechanisms of formation: J. Geophys. Res., v. 107.

Fishbaugh, K.E., and Hvidberg, C., 2006, Martian North Polar Layered Deposits Stratigraphy: Implications for Accumulation rates and Flow: Journal of Geophysical Research-Planets, v. 111, p. 1-21.

Fisher, D.A., 1993, If Martian Ice Cap Flow: Ablation Mechanisms and Appearance: Icarus, v. 105, p. 501-511.

Frey, H.V., and Schultz, R.A., 1988, Large impact basins and the mega-impact origin for the crustal dichotomy on Mars: Geophysical Research Letters, v. 15, p. 229-32.

Gwinner, K., Scholten, F., Elgner, S.*, et al.*, 2007, Systematic mapping of Mars by HRSC DTM and Orthoimages: Specifications and results fot the first 6 months of the mission, European Mars Science and Exploration Conference: Mars Express & ExoMars: Noordwijk, the Netherlands.

Hartmann, W.K., 2005, Moons and Planets, Thomson Brooks/Cole, 456 p.

Hartmann, W.K., and Neukum, G., 2001, Cratering chronology and the evolution of Mars: Space Science Reviews, v. 96, p. 165-194.

Heggy, E., Clifford, S.M., Younsi, A., *et al.*, 2006, On the Dielectric Properties of Dust and Ice-dust Mixtures: Experimental Characterization of the Martian Polar Layered Deposits Analog Materials: Fourth Mars Polar Science Conference.

Heipke, C., Schmidt, R., Brand, R., *et al.*, 2004, Performance of Automatic Tie Point Extraction Using HRSC Imager of the Mars Express Mission: International Archives Photogrammetry Remote Sensing and Spatial Information Science v. 35, p. 846-851.

Herkenhoff, K.E., Byrne, S., Russell, P.S., *et al.*, 2007, Meter-Scale Morphology of the North Polar Region of Mars: Science, v. 317, p. 1711-1715.

Hobbs, M.E., Jhon, M.S., and Eyring, H., 1966, The dielectric constant of liquid water and various forms of ice according to significant structure theory: Proceedings of the National Academy of Sciences of the United States of America, v. 56, p. 31-38.

Holt, J.W., Safaeinili, A., Plaut, J.J., *et al.*, 2008, Radar Sounding Evidence for Buried Glaciers in the Southern Mid-Latitudes of Mars: Science, v. 322, p. 1235-1238.

Howard, A.D., 1978, Origin of the stepped topography of the Martian poles: Icarus, v. 34, p. 581-599.

Howard, A.D., Cutts, J.A., and Blasius, K.R., 1982, Stratigraphic relationships within Martian polar cap deposits: Icarus, v. 50, p. 161-215.

Kass, D.M., and Yung, Y.L., 1995, Loss of atmosphere from Mars due to solar wind-induced sputtering: Science, v. 268, p. 697-699.

King, E.C., Hindmarsh, R.C.A., and Stokes, C.R., 2009, Formation of mega-scale glacial lineations observed beneath a West Antarctic ice stream: Nature Geosci, v. advanced online publication.

Kleinhans, M.G., 2005, Flow discharge and sediment transport models for estimating a minimum timescale of hydrological activity and channel and delta formation on Mars: Journal of Geophysical Research-Planets, v. 110.

Laskar, J., Levrard, B., and Mustard, J.F., 2002, Orbital forcing of the martian polar layered deposits: Nature, v. 419, p. 375-377.

Levrard, B., Forget, F., Montmessin, F., *et al.*, 2007, Recent formation and evolution of northern Martian polar layered deposits as inferred from a Global Climate Model: Journal of Geophysical Research-Planets, v. 112, p. 1-18.

Masson, P., Carr, M.H., Costard, F., *et al.*, 2001, Geomorphologic Evidence for Liquid Water.

Milkovich, S.M., and Head, J.W., 2006, Surface texture of Mars' north polar layered deposits: A framework for interpretation and future exploration: Mars, v. 2, p. 21-45.

Milkovich, S.M., Plaut, J.J., Safaeinili, A., *et al.*, 2009, Stratigraphy of Promethei Lingula, south polar layered deposits, Mars, in radar and imaging data sets: J. Geophys. Res., v. 114.

Neukum, G., Ivanov, B.A., and Hartmann, W.K., 2001, Cratering Records in the Inner Solar System in Relation to the Lunar Reference System: Space Science Reviews, v. 96, p. 55-86.

Neukum, G., Jaumann, R., Basilevsky, A.T., *et al.*, 2009, Mars Express:

The Scientific Investigations; HRSC: High Resolution Stereo Camera, ESA Communication Production Office.

Ng, F.S.L., and Zuber, M.T., 2006, Pattering instability on the Mars polar ice caps: Journal of Geophysical Research-Planets, v. 111.

Oosthoek, J.H.P., and Kleuskens, M.H.P., 2009, 3D interpretation of SHARAD radargram data: 40th Lunar and Planetary Science Conference.

Peeples, W.J., Sill, W.R., May, T.W., *et al.*, 1978, Orbital radar evidence for lunar subsurface layering in Maria Serenitatis and Crisium: J. Geophys. Res., v. 83, p. 3459-3468.

Perron, J.T., and Huybers, P., 2009, Is there an orbital signal in the polar layered deposits on Mars?: Geology, v. 37, p. 155-158.

Phillips, R.J., Zuber, M.T., Smrekar, S.E., *et al.*, 2008, Mars north polar deposits: Stratigraphy, age, and geodynamical response: Science, v. 320, p. 1182-1185.

Picardi, G., Plaut, J.J., Biccari, D., *et al.*, 2005, Radar Soundings of the Subsurface of Mars: Science, v. 310, p. 1925-1928.

Plaut, J.J., Picardi, G., Safaeinili, A., *et al.*, 2007, Subsurface Radar Sounding of the South Polar Layered Deposits of Mars: Science, v. 316, p. 92-95.

Putzig, N.E., Phillips, R.J., Campbell, B.A., *et al.*, 2009a, Subsurface structure of Planum Boreum from Mars Reconnaissance Orbiter Shallow Radar soundings: Icarus, p. 34.

Putzig, N.E., Phillips, R.J., Campbell, B.A., *et al.*, 2009b, Subsurface structure of Planum Boreum from Mars Reconnaissance Orbiter Shallow Radar soundings: Icarus, v. In Press, Corrected Proof.

Rossi, A.P., 2008, HRSC Map & Reference issues: United States.

Scholten, F., Gwinner, K., Roatsch, T., *et al.*, 2005, Mars Express HRSC Data Processing - Methods and Operational Aspects: Photogrammetric Engineering & Remote Sensing, v. 71, p. 1143-1152.

Schorghofer, N., 2008, Temperature response of mars to Milankovitch cycles: Geophysical Research Letters, v. 35.

Schultz, P.H., 2007, PLANETARY SCIENCE: Hidden Mars: Science, v. 318, p. 1080-1081.

Scott, D.H., and Carr, M.H., 1978, Geologic map of Mars: U.S. Geological Survey Miscellaneous Investigations Series Map, v. I-803.

Seidelmann, P.K., Abalakin, V.K., Bursa, M., *et al.*, 2002, Report of the IAU/IAG working group on cartographic coordinates and rotational elements of the planets and satellites: 2000: Celestial Mechanics and Dynamical Astronomy, v. 82, p. 83-111.

Seu, R., Phillips, R.J., Alberti, G., *et al.*, 2007a, Accumulation and Erosion of Mars' South Polar Layered Deposits: Science, v. 317, p. 1715-1718.

Seu, R., Phillips, R.J., Biccari, D., *et al.*, 2007b, SHARAD sounding radar on the Mars Reconnaissance Orbiter: J. Geophys. Res., v. 112.

Siegert, M.J., and Kwok, R., 2000, Ice-sheet radar layering and the development of preferred crystal orientation fabrics between Lake Vostok and Ridge B, central East Antarctica: Earth and Planetary Science Letters, v. 179, p. 227-235.

Slavney, S., and Orosei, R., 2007, Mars Reconnaissance Orbiter: Shallow radar reduced data record software interface specification, p. 1-49.

Sleep, N.H., 1994, Martian plate tectonics: J. Geophys. Res., v. 99, p. 5639-5655.

Smith, D.E., Neumann, G.A., and Zuber, M.T., 2003, Mars Orbiter Laser Altimeter; Mola Precision Experiment Data Record Software Interface Specification (Mola PEDR SIS).

Smith, D.E., Zuber, M.T., Solomon, S.C., *et al.*, 1999, The Global Topography of Mars and Implications for Surface Evolution: Science, v. 284, p. 1495-1503.

Smith, D.E., Zuber, M.T., Torrence, M.H., *et al.*, 2009, Time variations of Mars' gravitational field and seasonal changes in the masses of the polar ice caps: Journal of Geophysical Research-Planets, v. 114.

Tanaka, K.L., 2005, Geology and insolation-driven climatic history of Amazonian north polar materials on Mars: Nature, v. 437, p. 991-994.

Tanaka, K.L., Rodriguez, J.A.P., Skinner, J.A., *et al.*, 2008, North polar region of Mars: Advances in stratigraphy, structure, and erosional modification, p. 318-358.

Tanaka, K.L., and Scott, D.H., 1987, Geologic map of the polar regions of Mars: U.S. Geological Survey Miscellaneous Investigations Series Map.

Watters, T.R., Campbell, B., Carter, L., *et al.*, 2007, Radar Sounding of the Medusae Fossae Formation Mars: Equatorial Ice or Dry, Low-Density Deposits?: Science, v. 318, p. 1125-1128.

Watters, T.R., Leuschen, C.J., Plaut, J.J., *et al.*, 2006, MARSIS radar sounder evidence of buried basins in the northern lowlands of Mars: Nature, v. 444, p. 905-908.

Weijermars, R., 1986, The polar spirals of Mars may be due to glacier surges deflected by Coriolis forces: Earth and Planetary Science Letters, v. 76, p. 227-240.

Wilhelms, D.E., and Squyres, S.W., 1984, The Martian hemisphere dichotomy may be due to a giant impact: Nature, v. 309, p. 138-40.

Winebrenner, D.P., Koutnik, M.R., Waddington, E.D., *et al.*, 2008, Evidence for ice flow prior to trough formation in the martian north polar layered deposits: Icarus, v. 195, p. 90-105.

Zeng, Z., Xie, H., Birnbaum, S.J., *et al.*, 2007, New Insight on the Origin of Spiral Troughs in Martian Polar Ice Caps: 7th International Conference on Mars, p. 3368.